

Weak charged and neutral current induced one pion production off the nucleon

M. Rafi Alam,¹ M. Sajjad Athar,¹ S. Chauhan*,¹ and S. K. Singh¹

¹*Department of Physics, Aligarh Muslim University, Aligarh - 202 002, India*

We present a study of neutrino/antineutrino induced charged and neutral current single pion production off the nucleon. For this, we have considered $P_{33}(1232)$ resonance, non-resonant background terms, other higher resonances like $P_{11}(1440)$, $S_{11}(1535)$, $D_{13}(1520)$, $S_{11}(1650)$ and $P_{13}(1720)$. For the non-resonant background terms a microscopic approach based on SU(2) non-linear sigma model has been used. The vector form factors for the resonances are obtained by using the relationship between the electromagnetic resonance form factors and helicity amplitudes provided by MAID. Axial coupling $C_5^A(0)$ in the case of $P_{33}(1232)$ resonance is obtained by fitting the ANL and BNL ν -deuteron reanalyzed scattering data. The results are presented with and without deuteron effect for the total scattering cross sections for all possible channels viz. $\nu_l(\bar{\nu}_l) + N \rightarrow l^-(l^+) + N' + \pi^i$; $\nu_l(\bar{\nu}_l) + N \rightarrow \nu_l(\bar{\nu}_l) + N' + \pi^i$, where $N, N' = p, n$, $\pi^i = \pi^\pm$ or π^0 and $l = e, \mu$.

PACS numbers: 13.15.+g, 12.15.-y, 12.39.Fe

I. INTRODUCTION

A precise knowledge of (anti)neutrino-nucleus cross sections is an important input in minimizing the systematic errors in the analysis of (anti)neutrino oscillation experiments. Most of these experiments are presently being done in the (anti)neutrino energy region of a few GeV. In this energy region of accelerator experiments like MiniBooNE [1–4], T2K [5, 6], NO ν A [7], MicroBooNE [8], ArgoNeuT [9, 10], LBNO [11], MINOS [12], DUNE [13], etc. major contribution to the neutrino-nucleus cross section comes from the quasielastic process and the inelastic process of single pion production(SPP). The basic reaction mechanism for quasielastic process is widely studied in the Standard Model and there exist many calculations of nuclear medium effects(NME) using various nuclear models which have been summarized recently in several review articles [14–18]. In the case of single pion production processes from nuclear target, nuclear medium effects play an important role in the production process. In addition to this, the produced pion, being a hadron interacts with the residual nucleus. These pions may get absorbed in the nucleus or may change their charge state through charge exchange pion nucleon scattering processes like $\pi^- + p \rightarrow \pi^0 + n$, $\pi^0 + p \rightarrow \pi^+ + n$, etc. Therefore, the final state interaction(FSI) effect of the pion with the nucleus has also to be taken into account. Moreover, presently there is lack of consensus on theoretical modeling of basic reaction mechanism of (anti)neutrino induced single pion production from free nucleons.

At neutrino energies of ~ 1 GeV, the single pion production channels make a significant contribution to the cross section for charged lepton production and are important processes to be considered in the analysis of oscillation experiments which select charged current inclusive events as signal. In experiments which select the quasielastic production of charged leptons as signals for the analysis of oscillation experiments, single pion production channel gives rise to background contribution. For example, neutral current induced neutral pion production is a background to ν_e -appearance oscillation experiments while charged current events producing charged pions contribute to background in ν_μ -disappearance experiments. It is, therefore, very important to theoretically understand and model the single pion production processes on nuclear targets like ^{12}C , ^{16}O , ^{40}Ar , ^{56}Fe , ^{208}Pb , which are being used in the present experiments.

The present attempts to explain the experimental data on weak pion production in neutrino/antineutrino reactions from nucleons bound inside the nucleus like the experiments performed at MiniBooNE [1–4], SciBooNE[4], K2K[19–22] and more recently from MINER ν A collaboration[23–27] have highlighted the inadequacy of our present understanding of nuclear medium and final state interaction effects. The experimental results of single pion production and their comparison with the various theoretical calculations have also necessitated the need to re-examine the basic reaction mechanism for the production of single pion from free nucleon target.

The various possible reactions which may contribute to the single pion production either through charged current or neutral current neutrino/antineutrino induced reaction on a nucleon target are the following:

* Corresponding author: niharikavatsa21@gmail.com

Charged current(CC) induced processes:

$$\begin{aligned}
 \nu_l p &\rightarrow l^- p \pi^+ & \bar{\nu}_l n &\rightarrow l^+ n \pi^- \\
 \nu_l n &\rightarrow l^- n \pi^+ & \bar{\nu}_l p &\rightarrow l^+ p \pi^- \\
 \nu_l n &\rightarrow l^- p \pi^0 & \bar{\nu}_l p &\rightarrow l^+ n \pi^0
 \end{aligned}
 \quad ; \quad l = e, \mu \quad (1)$$

and neutral current(NC) induced processes:

$$\begin{aligned}
 \nu_l p &\rightarrow \nu_l n \pi^+ & \bar{\nu}_l p &\rightarrow \bar{\nu}_l p \pi^0 \\
 \nu_l p &\rightarrow \nu_l p \pi^0 & \bar{\nu}_l p &\rightarrow \bar{\nu}_l n \pi^+ \\
 \nu_l n &\rightarrow \nu_l n \pi^0 & \bar{\nu}_l n &\rightarrow \bar{\nu}_l n \pi^0 \\
 \nu_l n &\rightarrow \nu_l p \pi^- & \bar{\nu}_l n &\rightarrow \bar{\nu}_l p \pi^-
 \end{aligned} \quad (2)$$

The existing experimental data on single pion production process from (almost)free nucleons are available only from the old bubble chamber experiments performed at ANL [28] and BNL [29] from deuteron/hydrogen targets. These data on $\nu_\mu p \rightarrow \mu^- p \pi^+$ differ with each other by about 30–40% which has been attributed in the past to different flux normalization in these experiments. These data, when used to fix various parameters of theoretical models of reaction mechanisms for single pion production, give rise to considerable uncertainties in the determination of these parameters, which in turn lead to higher uncertainties in predicting the single pion production cross section from nuclear targets. Recently reanalysis of the old bubble chamber data by the two independent groups have tried to arrive at a consistent set of data from ANL [28] and BNL [29] experiments either by minimizing the neutrino flux uncertainties [30, 31] or by reconstructing the data using the cross section ratio for single pion production to the quasielastic processes, and observed quasielastic cross sections [32]. It is hoped that the use of reanalyzed/reconstructed data on free nucleon targets will help towards a better understanding of pion production reaction mechanism. Furthermore, using these data a better determination of various parameters to be used in the theoretical calculations may also be possible.

Theoretically, the weak single pion production has been studied for almost 50 years. The early calculations were based on dynamical models using dispersion theory or quark models or an effective Lagrangian field theory [33–38] and a comprehensive summary has been given by C. H. Llewellyn Smith [39]. Since then calculations have been made either by using quark models [40–45] or dynamical models [46–48], but most of the recent calculations have been done using effective Lagrangian field theory [49–54], where the calculations are performed using a $\Delta(1232)$ dominance model to successfully explain the experimental data on $\nu_\mu p \rightarrow \mu^- p \pi^+$ channel by fitting the $N - \Delta$ transition form factors. These form factors are found to be consistent with the predictions of the hypothesis of conserved vector current(CVC) and partial conservation of axial vector current(PCAC). However, these analyses have large uncertainties mainly due to the incompatibility of single pion production data in this channel from ANL [28] and BNL [29] experiments which also reflect into the determination of $N - \Delta$ transition form factors. These uncertainties are further enhanced as systematic errors due to nuclear medium and FSI effects, which also come into play, when applied to explain the data from nuclear targets like ^{12}C , ^{16}O and other heavier nuclear targets.

The recent tension between the experimental results on pion production from ^{12}C nuclear target in the Mini-BooNE [1–4] and MINER ν A [23–27] experiments have also highlighted the inadequacy of our present theoretical understanding of single pion production processes from nuclear targets. One of the main concerns in the theoretical modeling of basic reaction mechanism for SPP is the role of non-resonant background terms and the contribution of higher resonances beyond the $\Delta(1232)$ dominance model.

The role of non-resonant background terms was also emphasized in earlier analyses of experimental data from ANL [28] and BNL [29] experiments. It was concluded that there might be a sizable contribution from the non-resonant background terms coming specially in neutrino-neutron channels like $\nu_\mu n \rightarrow \mu^- p \pi^0$ and $\nu_\mu n \rightarrow \mu^- n \pi^+$, even though they may be small in $\nu_\mu p \rightarrow \mu^- p \pi^+$ channel. Indeed a theoretical calculation by Fogli and Nardulli[55, 56] in an effective Lagrangian field theoretical model has shown that the inclusion of pion pole, nucleon pole, and other $I = \frac{1}{2}$ resonance contribution leads to a better explanation of ANL [28], BNL [29] and CERN [57–59] data.

In recent times, the need for inclusion of non-resonant and resonant ($I = \frac{1}{2}$ channel) background terms to the dominant $\Delta(1232)$ contributions to explain the neutrino induced single pion production has been emphasized by many authors[53, 60–63] and numerical calculations have been performed to explain the present data. These calculations have been done either phenomenologically [61–63] or in an effective Lagrangian field theoretical model[53, 60]. However, there is no consensus on the treatment of background terms whether they should be added coherently or incoherently to the dominant $\Delta(1232)$ contribution. It is also of crucial importance to understand the background contribution, to determine the $N - \Delta$ transition form factors in $\nu_\mu p \rightarrow \mu^- p \pi^+$ and $\bar{\nu}_\mu n \rightarrow \mu^+ n \pi^-$ channels which are dominated by $\Delta(1232)$ - excitation and its subsequent decay to pions and to interpret present and future data in (anti)neutrino-nucleon channels like $\nu_\mu n \rightarrow \mu^- p \pi^0$, $\nu_\mu n \rightarrow \mu^- n \pi^+$, $\bar{\nu}_\mu p \rightarrow \mu^+ n \pi^0$ and $\bar{\nu}_\mu p \rightarrow \mu^+ p \pi^-$. A theoretical

understanding of presently reported data [32] from reanalysis/reconstruction of ANL [28] and BNL [29] data set in a chiral invariant effective Lagrangian field theoretical model using $\Delta(1232)$ dominance and non-resonant background terms will be highly useful for the purpose of determining various parameters like $N-\Delta$ transition form factors, needed to describe the basic reaction mechanism of single pion production and its application to study nuclear medium and FSI effects.

In this paper, we have presented the results for the total scattering cross sections for pion production from nucleons. The effect of using deuteron target also have been taken into account in a simple model. We have studied single pion production from free nucleons in a model which goes beyond the $\Delta(1232)$ dominance model and include the non-resonant contribution from pion pole, nucleon pole and contact terms calculated in a chiral invariant field theoretical model. The contributions of $I = \frac{1}{2}$ resonances like $P_{11}(1440)$, $D_{13}(1520)$, $S_{11}(1535)$, $S_{11}(1650)$ and $P_{13}(1720)$ in second resonance region are also taken into account using a phenomenological Lagrangian. The role of interference between non-resonant and $\Delta(1232)$ dominant terms is studied. The results are compared with the reconstructed data of ANL and BNL experiments reanalyzed by Wilkinson et al. [32] on $\nu_\mu p \rightarrow \mu^- p \pi^+$ channel to fix the $N-\Delta$ transition form factors and have been applied to study all the pion production channels from proton and neutron targets which are induced by charged and neutral weak currents with neutrino and antineutrino beams. We have also performed calculations using different cuts on center of mass energy i.e. ($W < 1.4\text{GeV}$ and 1.6GeV) and compared our results with the available results of ANL [28] and BNL [29] experiments. For the charged current antineutrino induced $\bar{\nu}_\mu n \rightarrow \mu^+ n \pi^-$ and $\bar{\nu}_\mu p \rightarrow \mu^+ p \pi^-$ processes, we have compared our results with the available results of Bolognese et al. [64]. For neutral current neutrino induced process $\nu_l n \rightarrow \nu_l p \pi^-$, we have compared the present results with the results of Derrick et al. [65].

In section-II, we present the formalism in brief and discuss the non-resonant background mechanism in section-II A for charged as well as neutral current induced processes. While the resonant mechanism are separately discussed in section-II B for charged and in section-II C for neutral current pion production processes. The results and their discussions are presented in section-III. Finally, we conclude the findings in section-IV.

II. FORMALISM

The differential scattering cross section for the processes mentioned in Eqs. 1 and 2, may be written as

$$d\sigma = \frac{1}{4\sqrt{(k \cdot p)^2 - m_\nu^2 M^2} (2\pi)^5} \frac{d\vec{k}'}{(2E_l)} \frac{d\vec{p}'}{(2E_p)} \frac{d\vec{k}_\pi}{(2E_\pi)} \delta^4(k + p - k' - p' - k_\pi) \bar{\Sigma} \Sigma |\mathcal{M}|^2, \quad (3)$$

where $k(k')$ is the four momentum of the incoming(outgoing) lepton having energy $E(E')$ while $p(p')$ is the four momentum of the incoming(outgoing) nucleon and the pion momentum is k_π having energy E_π . m_ν is the neutrino mass and M is the nucleon mass. $\bar{\Sigma} \Sigma |\mathcal{M}|^2$ is the square of the transition amplitude averaged(summed) over the spins of the initial(final) state and may be written as

$$\mathcal{M} = \frac{G_F}{\sqrt{2}} j_\mu^{(L)} j^\mu{}^{(H)}, \quad (4)$$

where $j_\mu^{(L)}$ and $j^\mu{}^{(H)}$ are the leptonic and hadronic currents, respectively and G_F is the Fermi coupling constant($=1.166 \times 10^{-5} \text{GeV}^{-2}$). The weak leptonic current has $V-A$ structure and is written as

$$j_\mu^{(L)} = \bar{u}(k') \gamma_\mu (1 \pm \gamma_5) u(k), \quad (5)$$

where negative sign is for neutrino and positive sign stands for antineutrino induced processes. $j^\mu{}^{(H)}$ describes the hadronic matrix element for $W^i + N \rightarrow N' + \pi$ interaction and obtained using an effective Lagrangian for $W^i + N \rightarrow N' + \pi$ interaction for charged($W^i \equiv W^\pm$; $i = \pm$) and neutral current($W^i \equiv Z^0$; $i = 0$) induced processes. In this work, we extend our earlier calculations [49, 50, 66] which were performed in $\Delta(1232)$ dominance model by incorporating non-resonant background terms as well as higher resonant terms. The non-resonant background terms involve nucleon and pion poles and contact terms calculated using a chiral symmetric Lagrangian for describing their interactions which is obtained in a non-linear sigma model. The contribution of higher resonances lying in the second resonance region beyond the $\Delta(1232)$ resonance are also included as they may be important in the weak pion production induced by (anti)neutrinos of energy $E_{\nu(\bar{\nu})} < 2.0\text{GeV}$. In the following sections, we describe briefly the hadronic matrix element for non-resonant background terms, $\Delta(1232)$ resonance and higher resonances.

The Feynman diagrams which may contribute to the matrix element of the hadronic current are shown in Fig. 1. The non-resonant background terms include five diagrams viz, direct(NP) and cross nucleon pole(CP), contact term(CT),

pion pole(PP) and pion in flight(PF) terms. For $\Delta(1232)$ resonance we have included both direct(s-channel) and cross(u-channel) diagrams. Apart from $\Delta(1232)$ resonance, we have also taken contributions from $P_{11}(1440)$, $S_{11}(1535)$ and $S_{11}(1650)$ spin half resonances and $D_{13}(1520)$ and $P_{13}(1720)$ spin three-half resonances and considered both s-channel and u-channel contributions.

In the following sections, we present the formalism in brief which has been used for the non-resonant background terms and the resonant spin half and spin three-half contributions to the one pion production processes.

A. Non-resonant background contribution

The contribution from the non-resonant background terms in the case of charged($W^i \equiv W^\pm ; i = \pm$) and neutral($W^i \equiv Z^0 ; i = 0$) current reaction $W^i N \rightarrow N' \pi$ may be obtained using non-linear sigma model based on the works of Hernandez et al. [53]. In lowest order, the contributions to the hadronic current are written in a model independent way as

$$\begin{aligned}
j^\mu|_{NP} &= a \mathcal{A}^{NP} \bar{u}(\vec{p}') \not{k}_\pi \gamma_5 \frac{\not{p} + \not{q} + M}{(p+q)^2 - M^2 + i\epsilon} [V_N^\mu(q) - A_N^\mu(q)] u(\vec{p}), \\
j^\mu|_{CP} &= a \mathcal{A}^{CP} \bar{u}(\vec{p}') [V_N^\mu(q) - A_N^\mu(q)] \frac{\not{p}' - \not{q} + M}{(p'-q)^2 - M^2 + i\epsilon} \not{k}_\pi \gamma_5 u(\vec{p}), \\
j^\mu|_{CT} &= a \mathcal{A}^{CT} \bar{u}(\vec{p}') \gamma^\mu (g_A f_{CT}^V(Q^2) \gamma_5 - f_\rho ((q - k_\pi)^2)) u(\vec{p}), \\
j^\mu|_{PP} &= a \mathcal{A}^{PP} f_\rho ((q - k_\pi)^2) \frac{q^\mu}{m_\pi^2 + Q^2} \bar{u}(\vec{p}') \not{q} u(\vec{p}), \\
j^\mu|_{PF} &= a \mathcal{A}^{PF} f_{PF}(Q^2) \frac{(2k_\pi - q)^\mu}{(k_\pi - q)^2 - m_\pi^2} 2M \bar{u}(\vec{p}') \gamma_5 u(\vec{p}),
\end{aligned} \tag{6}$$

with $a = \cos \theta_C$ for charged current process and $a = 1$ for neutral current process. q is the four momentum transfer ($= k - k'$), $q^2 (= -Q^2) \leq 0$ and k_π is the pion momentum. M is the mass of nucleon and m_π is the mass of pion. The constant factor \mathcal{A}^i , $i = NP, CP, CT, PP$ and PF , and are tabulated in Table-I.

The vector($V_N^\mu(q)$) and axial vector($A_N^\mu(q)$) currents for nucleon pole diagrams in the case of charged and neutral current interactions are calculated neglecting second class currents and are given by,

$$V_N^\mu(q) = \tilde{f}_1(Q^2) \gamma^\mu + \tilde{f}_2(Q^2) i \sigma^{\mu\nu} \frac{q_\nu}{2M} \tag{7}$$

$$A_N^\mu(q) = \left(\tilde{f}_A(Q^2) \gamma^\mu + \tilde{f}_P(Q^2) \frac{q^\mu}{M} \right) \gamma^5, \tag{8}$$

where $\tilde{f}_{1,2}(Q^2)$ and $\tilde{f}_{A,P}(Q^2)$ are the vector and axial vector form factors for nucleons. In the case of charged current process, the form factors $\tilde{f}_{1,2}(Q^2)$ are expressed in terms of isovector($f_{1,2}^V(Q^2)$) form factors as:

$$\tilde{f}_{1,2}(Q^2) \longrightarrow f_{1,2}^V(Q^2) = f_{1,2}^p(Q^2) - f_{1,2}^n(Q^2), \tag{9}$$

where $f_i^{p,n}(Q^2)$; $i = 1, 2$ are the Dirac($i = 1$) and Pauli($i = 2$) form factors of nucleons. These form factors are in turn expressed in terms of the experimentally determined Sach's electric $G_E^{p,n}(Q^2)$ and magnetic $G_M^{p,n}(Q^2)$ form factors [67]. While in the case of neutral current process, the form factors are expressed as:

$$\begin{aligned}
\tilde{f}_{1,2}(Q^2) &\xrightarrow{\text{for p}} \tilde{f}_{1,2}^p(Q^2) = \left(\frac{1}{2} - 2 \sin^2 \theta_W \right) f_{1,2}^p(Q^2) - \frac{1}{2} f_{1,2}^n(Q^2) \\
\tilde{f}_{1,2}(Q^2) &\xrightarrow{\text{for n}} \tilde{f}_{1,2}^n(Q^2) = \left(\frac{1}{2} - 2 \sin^2 \theta_W \right) f_{1,2}^n(Q^2) - \frac{1}{2} f_{1,2}^p(Q^2).
\end{aligned} \tag{10}$$

where θ_W is the Weinberg angle. On the other hand, the axial form factor($\tilde{f}_A(Q^2)$) is generally taken to be of dipole form and is given by

$$\tilde{f}_A(Q^2) = f_A(Q^2) = f_A(0) \left[1 + \frac{Q^2}{M_A^2} \right]^{-2}, \tag{11}$$

for charged current and by

$$\tilde{f}_A(Q^2) = \tilde{f}_A^{p,n}(0) \left[1 + \frac{Q^2}{M_A^2} \right]^{-2}, \quad (12)$$

for neutral current. Here $f_A(0)$ is the axial charge and is obtained from the quasielastic neutrino and antineutrino scattering as well as from the pion electro-production data. We have used $f_A(0)=-1.267$ and the axial dipole mass $M_A=1.026\text{GeV}$, which is the world average value [68], in the numerical calculations. For the neutral current induced reaction, $\tilde{f}_A^{p,n}(Q^2) = \pm \frac{1}{2}f_A(Q^2)$, where the plus(minus) sign stands for proton(neutron) target.

The next contribution from the axial part comes from the pseudoscalar form factor $\tilde{f}_P(Q^2)(=f_P(Q^2))$, the determination of which is based on PCAC and pion pole dominance and is related to $f_A(Q^2)$ through the relation

$$f_P(Q^2) = \frac{2M^2 f_A(Q^2)}{m_\pi^2 + Q^2}. \quad (13)$$

The contribution of this form being proportional to lepton mass vanishes for the neutral current processes. The hadronic current for NC processes have the contribution only from nucleon pole terms(s and u channels), while CC processes have contribution from all the diagrams viz. NP, CP, CT, PP and PF terms.

In order to conserve vector current for CC processes at the weak vertex, the two form factors viz. $f_{PF}(Q^2)$ and $f_{CT}^V(Q^2)$ are expressed in terms of the isovector nucleon form factor as [53]

$$f_{PF}(Q^2) = f_{CT}^V(Q^2) = 2f_1^V(Q^2). \quad (14)$$

The $\pi\pi NN$ vertex has the dominant ρ -meson cloud contribution and following Ref. [53], we have introduced ρ -form factor ($f_\rho(Q^2)$) at $\pi\pi NN$ vertex and taken it to be of monopole form:

$$f_\rho(Q^2) = \frac{1}{1 + Q^2/m_\rho^2}; \quad \text{with } m_\rho = 0.776\text{GeV}. \quad (15)$$

$f_\rho(Q^2)$ also has been used with axial part of the CT diagram in order to be consistent with the assumption of PCAC.

In the next section, we will discuss the formalism for charged and neutral current neutrino(antineutrino) induced processes for pion production through resonance excitations.

B. Charged current neutrino(antineutrino) induced processes

Constant term \rightarrow	$\mathcal{A}(\text{CC } \nu)$			$\mathcal{A}(\text{CC } \bar{\nu})$			$\mathcal{A}(\text{NC } \nu(\bar{\nu}))$			
Final states \rightarrow	$p\pi^+$	$n\pi^+$	$p\pi^0$	$n\pi^-$	$n\pi^0$	$p\pi^-$	$n\pi^+$	$p\pi^0$	$p\pi^-$	$n\pi^0$
NP	0	$\frac{-ig_A}{\sqrt{2}f_\pi}$	$\frac{-ig_A}{f_\pi}$	0	$\frac{ig_A}{\sqrt{2}f_\pi}$	$\frac{-ig_A}{f_\pi}$	$\frac{-ig_A}{\sqrt{2}f_\pi}$	$\frac{-ig_A}{f_\pi}$	$\frac{-ig_A}{\sqrt{2}f_\pi}$	$\frac{ig_A}{f_\pi}$
CP	$\frac{-ig_A}{f_\pi}$	0	$\frac{ig_A}{\sqrt{2}f_\pi}$	$\frac{-ig_A}{f_\pi}$	$\frac{-ig_A}{\sqrt{2}f_\pi}$	0	$\frac{-ig_A}{\sqrt{2}f_\pi}$	$\frac{-ig_A}{f_\pi}$	$\frac{-ig_A}{\sqrt{2}f_\pi}$	$\frac{ig_A}{f_\pi}$
CT	$\frac{-i}{\sqrt{2}f_\pi}$	$\frac{i}{\sqrt{2}f_\pi}$	$\frac{i}{2f_\pi}$	$\frac{-i}{\sqrt{2}f_\pi}$	$\frac{i}{f_\pi}$	$\frac{i}{\sqrt{2}f_\pi}$	-	-	-	-
PP	$\frac{i}{\sqrt{2}f_\pi}$	$\frac{-i}{\sqrt{2}f_\pi}$	$\frac{-i}{2f_\pi}$	$\frac{i}{\sqrt{2}f_\pi}$	$\frac{i}{f_\pi}$	$\frac{-i}{\sqrt{2}f_\pi}$	-	-	-	-
PF	$\frac{-i}{\sqrt{2}f_\pi}$	$\frac{i}{\sqrt{2}f_\pi}$	$\frac{i}{2f_\pi}$	$\frac{-i}{\sqrt{2}f_\pi}$	$\frac{-i}{f_\pi}$	$\frac{-i}{\sqrt{2}f_\pi}$	-	-	-	-

TABLE I: The values of constant term(\mathcal{A}^i) appearing in Eq. 6, where i corresponds to the nucleon pole(NP), cross nucleon pole(CP), contact term(CT), pion pole(PP) and pion in flight(PF) terms. f_π is pion weak decay constant and g_A is axial nucleon coupling.

Furthermore, we have also studied the contribution of other higher resonances to the single pion production channel which may also contribute along with the dominant $\Delta(1232)$ resonance, formalism for which has been discussed in the next section.

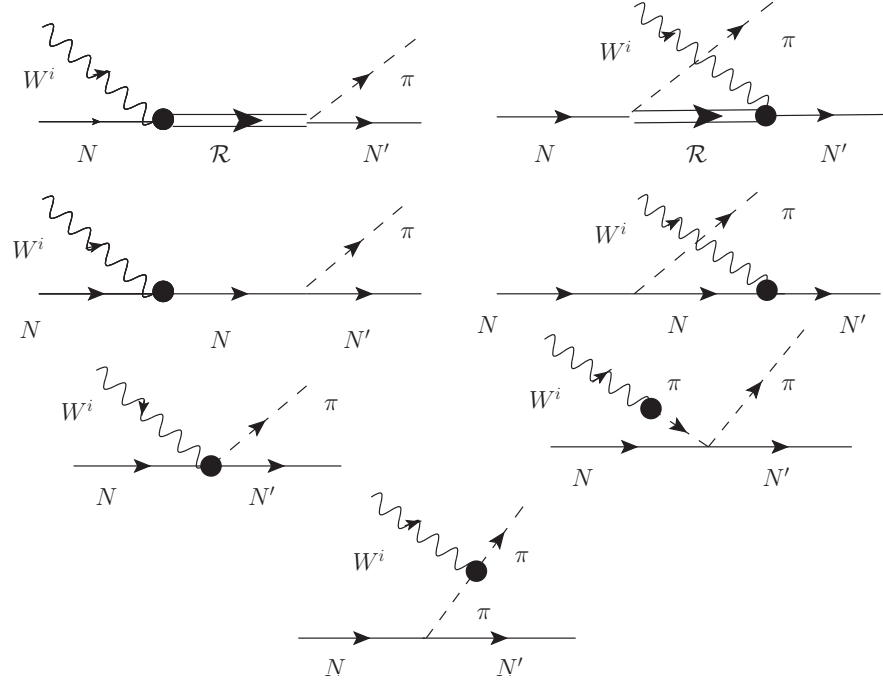


FIG. 1: Feynman diagrams contributing to the hadronic current corresponding to $W^i N \rightarrow N' \pi^{\pm,0}$, where ($W^i \equiv W^{\pm}$; $i = \pm$) for charged current processes and ($W^i \equiv Z^0$; $i = 0$) for neutral current processes with $N, N' = p$ or n . First row: direct and cross diagrams for resonance production where intermediate term \mathcal{R} stands for different resonances. Second row: nucleon pole (NP and CNP) terms. The contact term (CT) and pion pole (PP) term (third row left to right) and pion in flight (PF) (fourth row) contribute to the charged current processes only and do not contribute to the neutral current processes due to their symmetry properties.

1. Resonant Contribution

Besides the non-resonant background contribution to the pion production there are several resonances which may contribute along with the dominant $\Delta(1232)$ resonance channel. The basic neutrino(antineutrino) induced reactions for pion production through resonance excitations are the following:

$$\begin{aligned} \nu_l(k) + N(p) &\rightarrow l^-(k') + \mathcal{R}(p_R) \\ &\quad \searrow N'(p') + \pi(k_\pi) \end{aligned} \quad (16)$$

$$\begin{aligned} \bar{\nu}_l(k) + N(p) &\rightarrow l^+(k') + \mathcal{R}(p_R) \\ &\quad \searrow N'(p') + \pi(k_\pi) \end{aligned} \quad (17)$$

where \mathcal{R} stands for $\Delta(1232)$ and/or other higher resonances (R) which contribute to the pion production. In the next section, we briefly describe our model to include different resonances for the charged current and the neutral current induced reactions. In the present work, we have included six resonances, properties of which are summarized in Table-II. It may be noticed from the table that considered resonances are spin $\frac{3}{2}$ and spin $\frac{1}{2}$ resonant states with positive or negative parity. We shall discuss in brief the structure of the current for these two resonant states.

A. Spin $\frac{3}{2}$ resonances

The general structure for the hadronic current for spin three-half resonance excitation is determined by the following equation [39]

$$J_\mu^{\frac{3}{2}} = \bar{\psi}^\nu(p') \Gamma_{\nu\mu}^{\frac{3}{2}} u(p), \quad (18)$$

where $u(p)$ is the Dirac spinor for nucleon, $\psi^\mu(p)$ is the Rarita-Schwinger spinor for spin three-half particle and $\Gamma_{\nu\mu}^{\frac{3}{2}}$

has the following general structure for the positive and negative parity states :

$$\begin{aligned}\Gamma_{\nu\mu}^{\frac{3}{2}+} &= \left[V_{\nu\mu}^{\frac{3}{2}} - A_{\nu\mu}^{\frac{3}{2}} \right] \gamma_5 \\ \Gamma_{\nu\mu}^{\frac{3}{2}-} &= V_{\nu\mu}^{\frac{3}{2}} - A_{\nu\mu}^{\frac{3}{2}},\end{aligned}\quad (19)$$

where $V_{\frac{3}{2}}(A_{\frac{3}{2}})$ is the vector(axial-vector) current for spin three-half resonances. The vector and the axial-vector part of the currents are given by

$$\begin{aligned}V_{\nu\mu}^{\frac{3}{2}} &= \left[\frac{\tilde{C}_3^V}{M}(g_{\mu\nu}\not{q} - q_\nu\gamma_\mu) + \frac{\tilde{C}_4^V}{M^2}(g_{\mu\nu}q \cdot p' - q_\nu p'_\mu) + \frac{\tilde{C}_5^V}{M^2}(g_{\mu\nu}q \cdot p - q_\nu p_\mu) + g_{\mu\nu}\tilde{C}_6^V \right] \\ A_{\nu\mu}^{\frac{3}{2}} &= - \left[\frac{\tilde{C}_3^A}{M}(g_{\mu\nu}\not{q} - q_\nu\gamma_\mu) + \frac{\tilde{C}_4^A}{M^2}(g_{\mu\nu}q \cdot p' - q_\nu p'_\mu) + \tilde{C}_5^A g_{\mu\nu} + \frac{\tilde{C}_6^A}{M^2}q_\nu q_\mu \right] \gamma_5\end{aligned}\quad (20)$$

where \tilde{C}_i^V and \tilde{C}_i^A are the vector and axial charged current transition form factors which are functions of Q^2 .

From the conserved vector current hypothesis one takes $\tilde{C}_6^V(Q^2) = 0$. First, we shall discuss the expression of the form factors for the $\Delta(1232)$ resonance and write $\tilde{C}_i^V = C_i^V$ and $\tilde{C}_i^A = C_i^A$. Now for the $\Delta(1232)$ resonance, the other three vector form factors $C_i^V, i = 3, 4, 5$ are given in terms of the isovector electromagnetic form factors for $p \rightarrow \Delta^+$ transition and the parameterization of which are taken from the Ref. [69],

$$\begin{aligned}C_3^V(Q^2) &= \frac{2.13}{(1 + Q^2/M_V^2)^2} \times \frac{1}{1 + \frac{Q^2}{4M_V^2}}, \\ C_4^V(Q^2) &= \frac{-1.51}{(1 + Q^2/M_V^2)^2} \times \frac{1}{1 + \frac{Q^2}{4M_V^2}}, \\ C_5^V(Q^2) &= \frac{0.48}{(1 + Q^2/M_V^2)^2} \times \frac{1}{1 + \frac{Q^2}{0.776M_V^2}}\end{aligned}\quad (21)$$

with the vector dipole mass taken as $M_V = 0.84$ GeV.

The axial vector form factors $C_i^A(Q^2)$, ($i = 3, 4, 5$) are generally determined by using the hypothesis of PCAC with pion pole dominance through the off diagonal Goldberger-Trieman relation or obtained in quark model calculations [70, 71]. The early analysis of weak pion production experiments at ANL [28] and BNL [29] used Adler's model [72] as developed by Schreiner and von Hippel [40] to determine these form factors which are consistent with the hypothesis of PCAC and generalized Goldberger-Trieman relation. These considerations give $C_6^A(Q^2)$ in terms of $C_5^A(Q^2)$ and $C_5^A(0)$ in terms of $f_{\Delta N\pi}$ as:

$$C_6^A(Q^2) = C_5^A(Q^2) \frac{M^2}{Q^2 + m_\pi^2} \quad (22)$$

$$C_5^A(0) = f_\pi \frac{f_{\Delta N\pi}}{2\sqrt{3}M}, \quad (23)$$

where $f_{\Delta N\pi}$ is the $\Delta N\pi$ coupling strength for $\Delta \rightarrow N\pi$ decay.

The Q^2 dependence of $C_3^A(Q^2)$ and $C_4^A(Q^2)$ are obtained in Adler's model as [40, 72]

$$C_4^A(Q^2) = -\frac{1}{4}C_5^A(Q^2); \quad C_3^A(Q^2) = 0. \quad (24)$$

The Q^2 dependence of C_5^A is parameterized by Schreiner and von Hippel [40] in the Adler's model [72] and is given by

$$C_5^A(Q^2) = \frac{C_5^A(0) \left(1 + \frac{aQ^2}{b + Q^2}\right)}{(1 + Q^2/M_{A\Delta}^2)^2} \quad (25)$$

with a and b are determined from the experiments and found to be $a = -1.21$ and $b = 2$ [28, 73]. $M_{A\Delta}$ is the axial dipole mass.

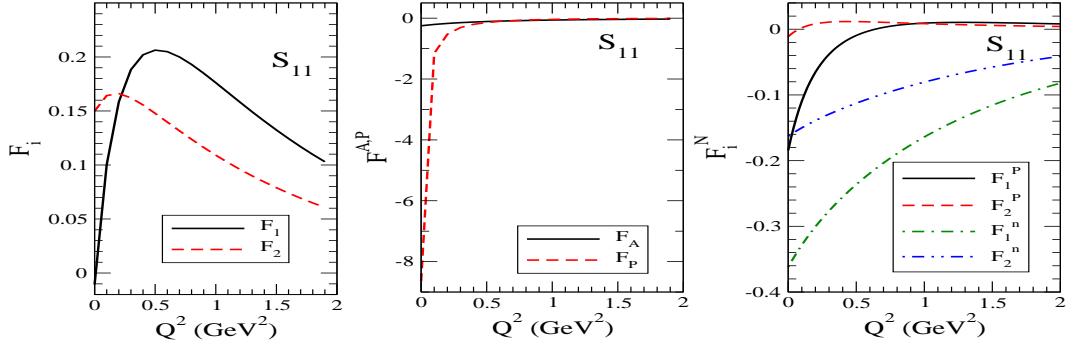


FIG. 2: Q^2 dependence of different form factors of S_{11} resonance. In the left panel the form of isovector form factors F_1^V and F_2^V are shown the form of which are given in Eq. 38. In the middle panel we have shown the axial form factors $F_{A,P}$ where for F_A we took the dipole form and the F_P is obtained from Eq. 41. In the right panel we have shown the explicit dependence of $F_i^{p,n}$, $i = 1, 2$ which may be obtained from the helicity amplitudes as given in Eq. 39.

The axial vector form factors as discussed in Eqs.22 and 25 along with the vector form factors given in Eq.21, have been used to analyze the present experimental cross sections for weak pion production. Most of the recent theoretical calculations [52–54, 69] use a simpler modification to the dipole form viz.

$$C_5^A(Q^2) = \frac{C_5^A(0)}{(1 + Q^2/M_{A\Delta}^2)^2} \frac{1}{1 + Q^2/(3M_{A\Delta}^2)}. \quad (26)$$

With the non-vanishing axial vector form factors determined in terms of $C_5^A(Q^2)$ and the vector form factors determined from electron scattering experiments, the weak pion production cross section is described in terms of $C_5^A(Q^2)$ with the parameters $C_5^A(0)$ and axial mass $M_{A\Delta}$. We chose $M_{A\Delta} = 1.026\text{GeV}$ corresponding to the world average value obtained from the experimental analysis of quasielastic scattering events [68], and then vary $C_5^A(0)$ to obtain a good description of reanalyzed data [32] of ANL and BNL experiments for $\nu_\mu p \rightarrow \mu^- p \pi^+$ reaction. While fitting the reanalyzed data for the reaction $\nu_\mu p \rightarrow \mu^- p \pi^+$, the contributions to the cross section is predominantly obtained from $\Delta(1232)$ resonant terms and the background terms have a little contribution. This has been further discussed in Section III.

One may write the most general form of the hadronic current for the s-channel(direct diagram) and u-channel(cross diagram) processes where a resonant state $R^{\frac{3}{2}}$ is produced and decays to a pion in the final state as

$$\begin{aligned} j^\mu \Big|_R^{\frac{3}{2}} &= i a \mathcal{C}^{\mathcal{R}} \frac{k_\pi^\alpha}{p_R^2 - M_R^2 + i M_R \Gamma_R} \bar{u}(\vec{p}') P_{\alpha\beta}^{3/2}(p_R) \Gamma_{\frac{3}{2}}^{\beta\mu}(p, q) u(\vec{p}), \quad p_R = p + q, \\ j^\mu \Big|_{CR}^{\frac{3}{2}} &= i a \mathcal{C}^{\mathcal{R}} \frac{k_\pi^\beta}{p_R^2 - M_R^2 + i M_R \Gamma_R} \bar{u}(\vec{p}') \hat{\Gamma}_{\frac{3}{2}}^{\mu\alpha}(p', -q) P_{\alpha\beta}^{3/2}(p_R) u(\vec{p}), \quad p_R = p' - q, \end{aligned} \quad (27)$$

where $a = \cos\theta_c$ for the charged current process and $a = 1$ for the neutral current process and $\mathcal{C}^{\mathcal{R}}$ is the coupling strength for $\mathcal{R} \rightarrow N\pi$, $\mathcal{R} \equiv \Delta$ or any other resonance R , determined from partial decay widths. M_R is the mass of resonance and Γ_R is the resonant decay width. These resonances are generally off-shell and their off-shell effects are also taken into account. $P_{\alpha\beta}^{3/2}$ is spin three-half projection operator and is given by

$$P_{\alpha\beta}^{3/2} = -(\not{p}' + M_R) \left(g_{\alpha\beta} - \frac{2}{3} \frac{p'_\alpha p'_\beta}{M_R^2} + \frac{1}{3} \frac{p'_\alpha \gamma_\beta - p'_\beta \gamma_\alpha}{M_R} - \frac{1}{3} \gamma_\alpha \gamma_\beta \right). \quad (28)$$

Apart from $\Delta(1232)$ resonance, we have also included other higher spin $\frac{3}{2}$ resonances like $D_{13}(1520)$ and $P_{13}(1720)$. The structure of the matrix element for the hadronic current is given in Eq. 27 and the weak vertex for positive and negative parity states are given in Eqs. 19. The vector and axial vector pieces are written in analogy with $\Delta(1232)$ resonance which are given in Eq. 20 with corresponding form factors, \tilde{C}_i^V and \tilde{C}_i^A , defined for each resonances.

The isovector \tilde{C}_i^V , $i = 3, 4, 5, 6$ form factors for $D_{13}(1520)$ and $P_{13}(1720)$, which have $J = \frac{3}{2}$, $I = \frac{1}{2}$, are written in terms of the charged and neutral form factors ($C_i^{p,n}(Q^2)$) through a simple relation [52],

$$\tilde{C}_i^V = C_i^p - C_i^n; \quad i = 3, 4, 5, 6. \quad (29)$$

The vector form factors $C_i^{p,n}(Q^2)$ are related with the helicity amplitudes for which the Q^2 dependence is parameterized as [74]

$$\mathcal{A}_\alpha(Q^2) = \mathcal{A}_\alpha(0)(1 + a_1 Q^2 + a_2 Q^4 + a_3 Q^6 + a_4 Q^8) e^{-b_1 Q^2} \quad (30)$$

where $\mathcal{A}_\alpha(Q^2)$ is the helicity amplitude; $A_{\frac{3}{2}(\frac{1}{2})}(Q^2)$ and/or $S_{\frac{1}{2}}(Q^2)$ and parameters $\mathcal{A}_\alpha(0)$ are generally determined by a fit to the photoproduction data of the corresponding resonance. While the parameters a_i ($i = 1 - 4$) and b_1 for each amplitude are obtained from electroproduction data available at different Q^2 .

The relations between the vector form factors $C_i^{p,n}(Q^2)$ and helicity amplitudes are given as [75]:

$$\begin{aligned} A_{\frac{3}{2}}^{p,n} &= \sqrt{\frac{\pi\alpha}{M} \frac{(M_R \mp M)^2 + Q^2}{M_R^2 - M^2}} \left[\frac{C_3^{p,n}}{M} (M \pm M_R) \pm \frac{C_4^{p,n}}{M^2} \frac{M_R^2 - M^2 - Q^2}{2} \right. \\ &\quad \left. \pm \frac{C_5^{p,n}}{M^2} \frac{M_R^2 - M^2 + Q^2}{2} \right] \\ A_{\frac{1}{2}}^{p,n} &= \sqrt{\frac{\pi\alpha}{3M} \frac{(M_R \mp M)^2 + Q^2}{M_R^2 - M^2}} \left[\frac{C_3^{p,n}}{M} \frac{M^2 + MM_R + Q^2}{M_R} - \frac{C_4^{p,n}}{M^2} \frac{M_R^2 - M^2 - Q^2}{2} \right. \\ &\quad \left. - \frac{C_5^{p,n}}{M^2} \frac{M_R^2 - M^2 + Q^2}{2} \right] \\ S_{\frac{1}{2}}^{p,n} &= \pm \sqrt{\frac{\pi\alpha}{6M} \frac{(M_R \mp M)^2 + Q^2}{M_R^2 - M^2} \frac{\sqrt{Q^4 + 2Q^2(M_R^2 + M^2) + (M_R^2 - M^2)^2}}{M_R^2}} \\ &\quad \times \left[\frac{C_3^{p,n}}{M} M_R + \frac{C_4^{p,n}}{M^2} M_R^2 + \frac{C_5^{p,n}}{M^2} \frac{M_R^2 + M^2 + Q^2}{2} \right], \end{aligned} \quad (31)$$

where $A_{\frac{3}{2},\frac{1}{2}}(Q^2)$ and $S_{\frac{1}{2}}(Q^2)$ are the amplitudes corresponding to the transverse and longitudinal polarizations, respectively and are parameterized at different Q^2 using Eq. 30. Once the parameters a_i and b_1 are fixed (Tables IV, V, VI) for $A_{\frac{3}{2},\frac{1}{2}}(Q^2)$ and $S_{\frac{1}{2}}(Q^2)$ amplitudes, one gets the form factors $C_i^{p,n}(Q^2)$.

The form factors $\tilde{C}_i^A(Q^2)$, ($i = 3, 4, 5, 6$) corresponding to the axial current have not been studied in the case of higher resonances. The earlier calculations have used PCAC to determine $\tilde{C}_5^A(Q^2)$ and $\tilde{C}_6^A(Q^2)$ and taken other form factors to be zero. In view of this, we have also taken a simple model for the determination of the axial form factors based on PCAC and Goldberger-Trieman relation and use the relation between $\tilde{C}_5^A(Q^2)$ and $\tilde{C}_6^A(Q^2)$ given in Eq. 22 to write $\tilde{C}_6^A(Q^2)$ in terms of $\tilde{C}_5^A(Q^2)$.

For $\tilde{C}_5^A(Q^2)$ a dipole form has been assumed

$$\tilde{C}_5^A(Q^2) = \frac{\tilde{C}_5^A(0)}{\left(1 + Q^2/M_A^{R^2}\right)^2} \quad (32)$$

with $\tilde{C}_5^A(0) = -2f_\pi \frac{f_{RN\pi}}{m_\pi}$, $f_{RN\pi}$ is the coupling for $R \rightarrow N\pi$ decay for each resonance R . M_A^R is taken as 1.026 GeV. The value of $\tilde{C}_5^A(0)$ for each resonance has been given in Table-2. $\tilde{C}_3^A(Q^2)$ as well as $\tilde{C}_4^A(Q^2)$ are taken as zero.

In the next section, we briefly discuss the inputs of hadronic current for spin $\frac{1}{2}$ resonance.

B. Spin $\frac{1}{2}$ resonances

The hadronic current for the spin $\frac{1}{2}$ resonant state is given by

$$j_{\frac{1}{2}}^\mu = \bar{u}(p') \Gamma_{\frac{1}{2}}^\mu u(p), \quad (33)$$

where $u(p)$ and $\bar{u}(p')$ are respectively the Dirac spinor and adjoint Dirac spinor for spin $\frac{1}{2}$ particle and $\Gamma_{\frac{1}{2}}^\mu$ is the vertex function which for a positive parity state is given by

$$\Gamma_{\frac{1}{2}+}^\mu = V_{\frac{1}{2}}^\mu - A_{\frac{1}{2}}^\mu \quad (34)$$

and for a negative parity is given by

$$\Gamma_{\frac{1}{2}-}^{\mu} = \left[V_{\frac{1}{2}}^{\mu} - A_{\frac{1}{2}}^{\mu} \right] \gamma_5 \quad (35)$$

where $V_{\frac{1}{2}}^{\mu}$ represents the vector current and $A_{\frac{1}{2}}^{\mu}$ represents the axial vector current.

These currents are parameterized in terms of vector($F_i(Q^2)$ ($i = 1, 2$)) and axial vector($F_A(Q^2)$ and $F_P(Q^2)$) form factors and are written as,

$$V_{\frac{1}{2}}^{\mu} = \left[\frac{F_1(Q^2)}{(2M)^2} (Q^2 \gamma^{\mu} + \not{q} q^{\mu}) + \frac{F_2(Q^2)}{2M} i \sigma^{\mu\alpha} q_{\alpha} \right] \gamma_5 \quad (36)$$

$$A_{\frac{1}{2}}^{\mu} = -F_A(Q^2) \gamma^{\mu} - \frac{F_P(Q^2)}{M} q^{\mu}, \quad (37)$$

where $F_i(Q^2)$ ($i = 1, 2$) are the isovector form factors which in turn are expressed in terms of Dirac and Pauli form factors for spin $\frac{1}{2}$ resonances for charged ($F_{1,2}^p$) and neutral ($F_{1,2}^n$) states:

$$F_i(Q^2) = F_i^p(Q^2) - F_i^n(Q^2), \quad i = 1, 2 \quad (38)$$

The form factors $F_i^{p,n}(Q^2)$ are derived from helicity amplitudes extracted from real and/or virtual photon scattering experiments.

The explicit relations between the form factors $F_i^{p,n}(Q^2)$ and the helicity amplitudes $A_{\frac{1}{2}}^{p,n}(Q^2)$ and $S_{\frac{1}{2}}^{p,n}(Q^2)$ are given by[63]

$$\begin{aligned} A_{\frac{1}{2}}^{p,n} &= \sqrt{\frac{2\pi\alpha}{M} \frac{(M_R \mp M)^2 + Q^2}{M_R^2 - M^2}} \left[\frac{Q^2}{4M^2} F_1^{p,n} + \frac{M_R \pm M}{2M} F_2^{p,n} \right] \\ S_{\frac{1}{2}}^{p,n} &= \mp \sqrt{\frac{\pi\alpha}{M} \frac{(M \pm M_R)^2 + Q^2}{M_R^2 - M^2} \frac{(M_R \mp M)^2 + Q^2}{4M_R M}} \left[\frac{M_R \pm M}{2M} F_1^{p,n} - F_2^{p,n} \right], \end{aligned} \quad (39)$$

where the upper sign represent the positive parity state and the lower sign denotes the negative parity state. M_R is the mass of corresponding resonance and $F_{1,2}^{p,n}(Q^2)$ are electromagnetic transition form factors. The Q^2 dependence of the helicity amplitudes is given by Eq. 30.

The axial current consists of two form factors viz. $F_A(Q^2)$ and $F_P(Q^2)$. The form factor $F_A(Q^2)$ and $F_P(Q^2)$ are determined assuming the the hypothesis of PCAC and pion pole dominance through the off diagonal Goldberger-Trieman relation for $N \rightarrow R$ transition, which gives

$$F_A(0) = -2f_{\pi} \frac{f_{R\frac{1}{2}}}{m_{\pi}}, \quad (40)$$

where $f_{R\frac{1}{2}}$ is the coupling strength for $R_{\frac{1}{2}} \rightarrow N\pi$ decay and $F_A(0)$ is the axial charge.

While the pseudoscalar form factor $F_P(Q^2)$ is related to the axial form factor $F_A(Q^2)$ via PCAC and is given by

$$F_P(Q^2) = \frac{(MM_R \pm M^2)}{m_{\pi}^2 + Q^2} F_A(Q^2) \quad (41)$$

where $+$ ($-$) sign is for positive(negative) parity resonances. The Q^2 dependence of the form factors thus obtained are shown in Figs. 2 and 3, respectively for $S_{11}(1650)$ and $P_{11}(1440)$ resonant states.

In analogy with Eq. 27, the most general form of the hadronic currents for the s-channel(direct diagram) and u-channel(cross diagram) processes where a resonant state $R_{\frac{1}{2}}$ is produced and decays to a pion in the final state, are written as

$$\begin{aligned} j^{\mu}|_R^{\frac{1}{2}} &= i a \mathcal{C}^{\mathcal{R}} \bar{u}(\vec{p}') \not{k}_{\pi} \gamma_5 \frac{\not{p} + \not{q} + M}{(p+q)^2 - M^2 + i\epsilon} \Gamma_{\frac{1}{2}}^{\mu} u(\vec{p}), \\ j^{\mu}|_{CR}^{\frac{1}{2}} &= i a \mathcal{C}^{\mathcal{R}} \bar{u}(\vec{p}') \Gamma_{\frac{1}{2}}^{\mu} \frac{\not{p}' - \not{q} + M}{(p'-q)^2 - M^2 + i\epsilon} \not{k}_{\pi} \gamma_5 u(\vec{p}), \end{aligned} \quad (42)$$

where $a = \cos\theta_c$ for the charged current process and $a = 1$ for the neutral current process. $\mathcal{C}^{\mathcal{R}}$ is a constant which includes the coupling strength, isopin factor involve in $\mathcal{R} \rightarrow N\pi$ transition, etc. This has been tabulated in Table-III. In the next section, we are going to present the method adopted to determine $\mathcal{R} \rightarrow N\pi$ coupling strength.

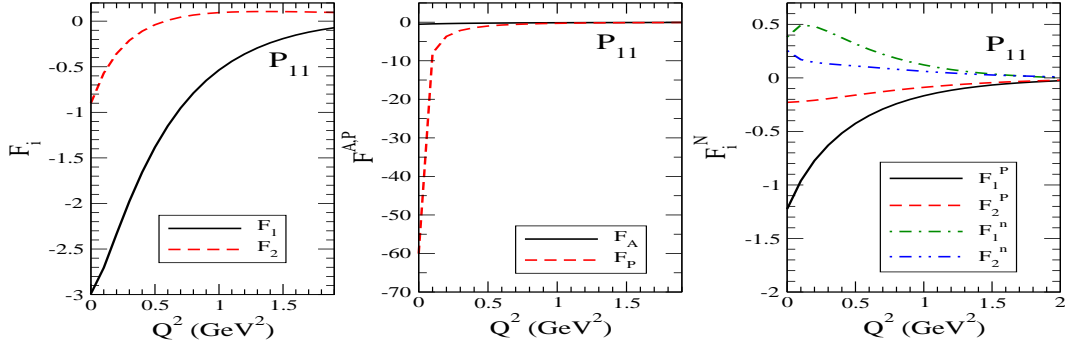


FIG. 3: Q^2 dependence of different form factors of $P_{11}(1440)$ resonance. The lines have same meaning as of Fig. 2.

2. Couplings of the resonances

Due to the lack of experimental data there is large uncertainty associated with $\mathcal{R}N\pi$ coupling at the $\mathcal{R} \rightarrow N\pi$ vertex. We have fixed $\mathcal{R}N\pi$ coupling using the data of branching ratio and decay width of these resonances from PDG [76] and use the expression for the decay rate which is obtained by writing the most general form of $\mathcal{R}N\pi$ Lagrangian,

$$\mathcal{L}_{R\frac{1}{2}N\pi} = \frac{f_{R\frac{1}{2}}}{m_\pi} \bar{\Psi}_{R\frac{1}{2}} \Gamma_{\frac{1}{2}}^\mu \partial_\mu \phi^i T_i \Psi \quad (43)$$

$$\mathcal{L}_{R\frac{3}{2}N\pi} = \frac{f_{R\frac{3}{2}}}{m_\pi} \bar{\Psi}_{R\frac{3}{2}} \Gamma_{\frac{3}{2}}^\mu \partial_\mu \phi^i T_i \Psi \quad (44)$$

where $f_{R\frac{1}{2}, R\frac{3}{2}}$ is the $\mathcal{R}N\pi$ coupling strength. Ψ is the nucleon field and $\Psi_{R\frac{1}{2}}$ and $\Psi_{R\frac{3}{2}}$ are the fields associated with the resonances of spin $\frac{1}{2}$ and spin $\frac{3}{2}$, respectively. ϕ^i are the pionic field and T_i are the isospin operator which is $T = \tau$ for isospin $\frac{1}{2}$ states and $T = T^\dagger$ for isospin $\frac{3}{2}$ states¹. The interaction vertex $\Gamma_{\frac{1}{2}}^\mu$ is $\gamma^\mu \gamma^5 (\gamma^\mu)$ for resonances (spin $\frac{1}{2}$) with positive (negative) parity. Similarly, the interaction vertex $\Gamma_{\frac{3}{2}}^\mu$ (spin $\frac{3}{2}$) is \mathbb{I}_4 for positive parity state and γ_5 for negative parity state. Using the above Lagrangian one may obtain the expression for the decay width in the resonance rest frame as

$$\Gamma_{R\frac{1}{2} \rightarrow \pi N} = \frac{\mathcal{C}}{4\pi} \left(\frac{f_{R\frac{1}{2}}}{m_\pi} \right)^2 (M_R \pm M)^2 \frac{E_N \mp M}{M_R} |\vec{q}_{cm}| \quad (45)$$

$$\Gamma_{R\frac{3}{2} \rightarrow \pi N} = \frac{\mathcal{C}}{12\pi} \left(\frac{f_{R\frac{3}{2}}}{m_\pi} \right)^2 \frac{E_N \pm M}{M_R} |\vec{q}_{cm}|^3, \quad (46)$$

where the upper(lower) sign represents the positive(negative) parity resonant state. The parameter \mathcal{C} is obtained from the isospin analysis and found out to be 3 for isospin $\frac{1}{2}$ state and 1 for isospin $\frac{3}{2}$ states. $|\vec{q}_{cm}|$ is the outgoing pion momentum measured from resonance rest frame and is given by,

$$|\vec{q}_{cm}| = \frac{\sqrt{(W^2 - m_\pi^2 - M^2)^2 - 4m_\pi^2 M^2}}{2M_R} \quad (47)$$

and E_N , the nucleon energy is

$$E_N = \frac{W^2 + M^2 - m_\pi^2}{2M_R}, \quad (48)$$

where W is the total center of mass energy carried by the resonance. In view of the above, we fix $N\Delta\pi$ coupling ($f_{\pi N\Delta}$)

¹ $\vec{\tau}$ and T^\dagger are the isospin operator for doublet and quartet, respectively.

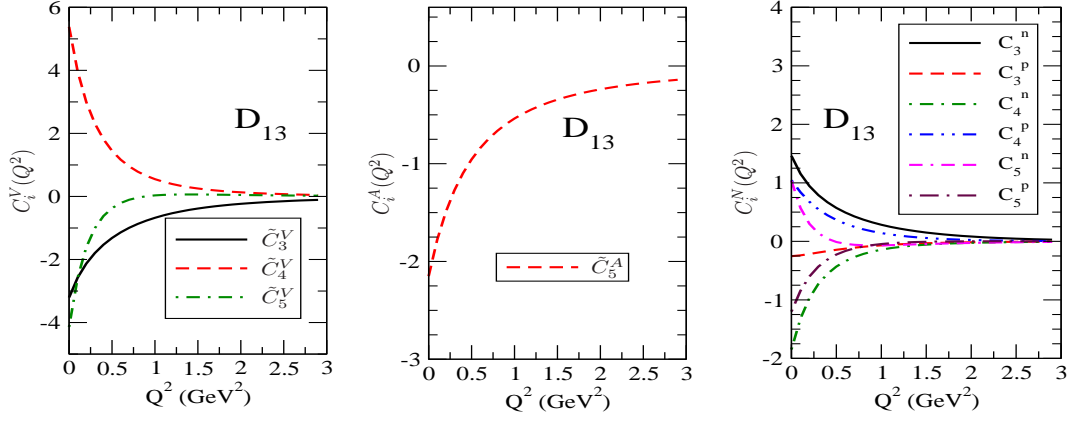


FIG. 4: Q^2 dependence of different form factors of D_{13} resonance. From left to right panel: \tilde{C}_3^V , \tilde{C}_4^V and \tilde{C}_5^V mentioned in Eq. 21, and \tilde{C}_5^A mentioned in Eq.32, and $C_i^{n,p}$, $i = 3, 4, 5$ mentioned in Eq. 29.

Resonances	M_R [GeV]	J	I	P	Γ_0^{tot} (GeV)	πN branching ratio (%)	$F_A(0)$ or $\tilde{C}_5^A(0)$	f^*
$P_{33}(1232)$	1.232	3/2	3/2	+	0.120	100	1.0	2.14
$P_{11}(1440)$	1.462	1/2	1/2	+	0.250	65	-0.43	0.215
$D_{13}(1520)$	1.524	3/2	1/2	-	0.110	60	-2.08	1.575
$S_{11}(1535)$	1.534	1/2	1/2	-	0.151	51	0.184	0.092
$S_{11}(1650)$	1.659	1/2	1/2	-	0.173	89	-0.21	-0.105
$P_{13}(1720)$	1.717	3/2	1/2	+	0.200	11	-0.195	0.147

TABLE II: Properties of the resonances included in the present model, with Breit-Wigner mass M_R , spin J, isospin I, parity P, the total decay width Γ_0^{tot} , the branching ratio into πN , the axial coupling ($F_A(0)$ for spin $\frac{1}{2}$ states; $C_5^A(0)$ for states with spin $\frac{3}{2}$) and f^* stands for $f_{R\frac{1}{2}}$ or $f_{R\frac{3}{2}}$ given in Eqs.43 and 44 and for $\Delta(1232)$ resonance $f^* = f_{\Delta N\pi}$.

by comparing $\Delta \rightarrow N\pi$ decay width evaluated in the rest frame of Δ ,

$$\Gamma_{\Delta}(s) = \frac{1}{6\pi} \left(\frac{f_{\pi N\Delta}}{m_{\pi}} \right)^2 \frac{M}{\sqrt{s}} \left[\frac{\lambda^{\frac{1}{2}}(s, m_{\pi}^2, M^2)}{2\sqrt{s}} \right]^3 \Theta(\sqrt{s} - M - m_{\pi}), \quad s = p_{\Delta}^2 \quad (49)$$

where $\lambda(x, y, z) = x^2 + y^2 + z^2 - 2xy - 2xz - 2yz$ is Källén function. To get the offshell effect of $\Delta(1232)$ resonance we have taken momentum dependent width. Using the above expressions for decay width the coupling for $\mathcal{R} \rightarrow N\pi$ are obtained and given in Table-II.

C. Neutral current neutrino(antineutrino) induced processes

In this section, we will briefly discuss the single pion production induced by neutral currents(NC1 π). Older data on NC1 π production are available from ANL [65] and Gargamelle [77] experiments. Recently, NC1 π production measurements have been performed by the MiniBooNE [78], K2K [79], SciBooNE [80] collaborations. The neutral current π^0 production in neutrino interactions plays an important role in the background studies of $\nu_{\mu} \leftrightarrow \nu_e$ or $\bar{\nu}_{\mu} \leftrightarrow \bar{\nu}_e$ oscillations in the appearance mode as well as in discriminating between $\nu_{\mu} \rightarrow \nu_{\tau}$ and $\nu_{\mu} \rightarrow \nu_s$ modes. Furthermore,

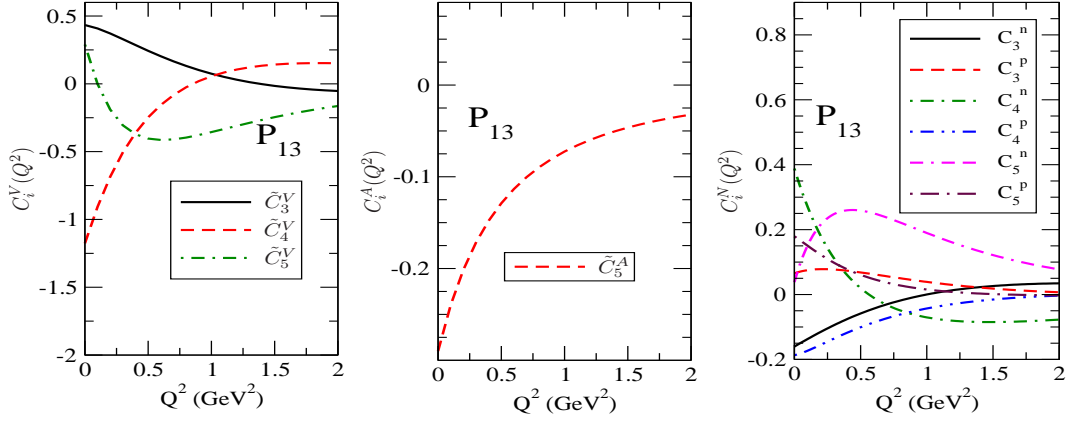


FIG. 5: Q^2 dependence of different form factors of P_{13} resonance. From left to right panel: \tilde{C}_3^V , \tilde{C}_4^V and \tilde{C}_5^V as mentioned in Eq. 21, \tilde{C}_5^A as mentioned in Eq.32 and C_i^N , $i = 3, 4, 5$ mentioned in Eq. 29.

TABLE III: Coupling constant($\mathcal{C}^{\mathcal{R}}$) for spin $\frac{1}{2}$ and spin $\frac{3}{2}$ resonances. Here f^* stands for $\mathcal{R} \rightarrow N\pi$ coupling which is for $\Delta(1232)$ resonance is $f_{\Delta N\pi}$ and $f_{R\frac{1}{2}}(f_{R\frac{3}{2}})$ for spin $\frac{1}{2}(\frac{3}{2})$ resonances given in Eqs.43 and 44.

Process	$\mathcal{C}^{\mathcal{R}}(\text{CC } \nu)$			$\mathcal{C}^{\mathcal{R}}(\text{CC } \bar{\nu})$		
	$p\pi^+$	$n\pi^+$	$p\pi^0$	$n\pi^-$	$n\pi^0$	$p\pi^-$
$P_{33}(1232)$	$\frac{\sqrt{3}f^*}{m_\pi}$	$\sqrt{\frac{1}{3}}\frac{f^*}{m_\pi}$	$-\sqrt{\frac{2}{3}}\frac{f^*}{m_\pi}$	$\frac{\sqrt{3}f^*}{m_\pi}$	$\sqrt{\frac{2}{3}}\frac{f^*}{m_\pi}$	$\sqrt{\frac{1}{3}}\frac{f^*}{m_\pi}$
$P_{11}(1440)$	0	$-\sqrt{\frac{1}{2}}\frac{f^*}{f_\pi}$	$-\frac{1}{2}\frac{f^*}{f_\pi}$	0	$-\frac{1}{2}\frac{f^*}{f_\pi}$	$\sqrt{\frac{1}{2}}\frac{f^*}{f_\pi}$
$D_{13}(1520)$	0	$-\sqrt{\frac{1}{2}}\frac{f^*}{m_\pi}$	$-\frac{1}{2}\frac{f^*}{m_\pi}$	0	$-\frac{1}{2}\frac{f^*}{m_\pi}$	$\sqrt{\frac{1}{2}}\frac{f^*}{m_\pi}$
$S_{11}(1535)$	0	$-\sqrt{\frac{1}{2}}\frac{f^*}{f_\pi}$	$-\frac{1}{2}\frac{f^*}{f_\pi}$	0	$-\frac{1}{2}\frac{f^*}{f_\pi}$	$\sqrt{\frac{1}{2}}\frac{f^*}{f_\pi}$
$S_{11}(1650)$	0	$-\sqrt{\frac{1}{2}}\frac{f^*}{f_\pi}$	$-\frac{1}{2}\frac{f^*}{f_\pi}$	0	$-\frac{1}{2}\frac{f^*}{f_\pi}$	$\sqrt{\frac{1}{2}}\frac{f^*}{f_\pi}$
$P_{13}(1720)$	0	$-\sqrt{\frac{1}{2}}\frac{f^*}{m_\pi}$	$-\frac{1}{2}\frac{f^*}{m_\pi}$	0	$-\frac{1}{2}\frac{f^*}{m_\pi}$	$\sqrt{\frac{1}{2}}\frac{f^*}{m_\pi}$

in the reconstruction of neutrino energy using quasielastic events like $\nu_e + n \rightarrow e^- + p$ or $\bar{\nu}_e + p \rightarrow e^+ + n$, a missing electron or positron in the π^0 decay may be mistaken as quasielastic event. Moreover, neutral current induced pion production may also help to distinguish between the production of ν_τ and $\bar{\nu}_\tau$ in some oscillation scenarios at neutrino energies much below the τ production threshold but above the pion threshold.

We have already discussed the contribution from non-resonant background terms for neutral current induced processes in section II A. Next we will present in brief the structure of resonant terms that may contribute to the hadronic current of (anti)neutrino induced neutral current processes.

1. Resonant contribution

The other higher resonances like $P_{11}(1440)$, $D_{13}(1520)$, $S_{11}(1535)$, $S_{11}(1650)$ and $P_{13}(1720)$, also contribute along with the dominant $\Delta(1232)$ resonance channel. The basic neutral current neutrino(antineutrino) induced reactions for pion production through resonance excitations are the following:

$$\begin{aligned} \nu_l(k) + N(p) &\rightarrow \nu_l(k') + \mathcal{R}(p_R) \\ &\quad \searrow N'(p') + \pi(k_\pi) \end{aligned} \quad (50)$$

$$\begin{aligned} \bar{\nu}_l(k) + N(p) &\rightarrow \bar{\nu}_l(k') + \mathcal{R}(p_R) \\ &\quad \searrow N'(p') + \pi(k_\pi) \end{aligned} \quad (51)$$

TABLE IV: MAID2008 parameterization of the transition form factors for proton target. $\bar{\mathcal{A}}_\alpha(0)$ is given in units of $10^{-3} \text{ GeV}^{-\frac{1}{2}}$ and the coefficients a_1, a_2, a_4, b_1 in units of $\text{GeV}^{-2}, \text{GeV}^{-4}, \text{GeV}^{-8}, \text{GeV}^{-2}$, respectively. For all fits $a_3 = 0$.

N^*, Δ^*	Amplitude	$\bar{\mathcal{A}}_\alpha(0)$	a_1	a_2	a_4	b_1
$P_{11}(1440)$	$A_{\frac{1}{2}}$	-61.4	0.871	-3.516	-0.158	1.36
	$S_{\frac{1}{2}}$	4.2	40.0	0	1.50	1.75
$D_{13}(1520)$	$A_{\frac{1}{2}}$	-27.4	8.580	-0.252	0.357	1.20
	$A_{\frac{3}{2}}$	160.6	-0.820	0.541	-0.016	1.06
	$S_{\frac{1}{2}}$	-63.5	4.19	0	0	3.40
$P_{13}(1720)$	$A_{\frac{1}{2}}$	73.0	1.89	0	0	1.55
	$A_{\frac{3}{2}}$	-11.5	10.83	-0.66	0	0.43
	$S_{\frac{1}{2}}$	-53.0	2.46	0	0	1.55

TABLE V: Maid2007 parameterization, Eq. (30), for proton target ($a_{2,3,4} = 0$).

N^*, Δ^*	Amplitude	$\bar{\mathcal{A}}_\alpha(0)$	a_1	b_1
$S_{11}(1535)$	$A_{\frac{1}{2}}$	66.4	1.608	0.70
	$S_{\frac{1}{2}}$	-2.0	23.9	0.81
$S_{11}(1650)$	$A_{\frac{1}{2}}$	33.3	1.45	0.62
	$S_{\frac{1}{2}}$	-3.5	2.88	0.76

where \mathcal{R} stands for the $\Delta(1232)$ and other higher resonances(R) which contribute to the pion production.

In the next section, we will briefly discuss formalism to include different resonances for the charged current and the neutral current processes.

A. Spin $\frac{3}{2}$ resonances

The general structure for the hadronic current $J_\mu^{\frac{3}{2}}$ for neutral current induced spin $\frac{3}{2}$ resonance in the intermediate state is given by Eq. 18, for which $\Gamma_{\nu\mu}^{\frac{3}{2}}$ is given by Eq. 19 for positive and negative parity states.

The vector and axial vector parts of the current(for $\Delta(1232)$, $I = \frac{3}{2}$) are given by Eq. 20 with the corresponding

TABLE VI: Maid2007 parameterization for neutron target($a_{2,3,4} = 0$).

N^*	Amplitude	$\bar{\mathcal{A}}_\alpha(0)$	a_1	b_1
$P_{11}(1440)$	$A_{\frac{1}{2}}$	54.1	0.95	1.77
	$S_{\frac{1}{2}}$	-41.5	2.98	1.55
$D_{13}(1520)$	$A_{\frac{1}{2}}$	-76.5	-0.53	1.55
	$A_{\frac{3}{2}}$	-154.0	0.58	1.75
	$S_{\frac{1}{2}}$	13.6	15.7	1.57
$S_{11}(1535)$	$A_{\frac{1}{2}}$	-50.7	4.75	1.69
	$S_{\frac{1}{2}}$	28.5	0.36	1.55
$S_{11}(1650)$	$A_{\frac{1}{2}}$	9.3	0.13	1.55
	$S_{\frac{1}{2}}$	10.	-0.5	1.55
$P_{13}(1720)$	$A_{\frac{1}{2}}$	-2.9	12.7	1.55
	$A_{\frac{3}{2}}$	-31.0	5.00	1.55
	$S_{\frac{1}{2}}$	0	0	0

neutral current form factors $(\tilde{C}_i^V)^{NC}$ ($i = 3, 4, 5$) and $(\tilde{C}_i^A)^{NC}$ ($i = 4, 5, 6$) which in the standard model are given in terms of \tilde{C}_i^V and \tilde{C}_i^A . The expressions given in Eq.20 now read as

$$(\tilde{C}_i^V)^{NC} \rightarrow (1 - 2\sin^2\theta_W)\tilde{C}_i^V, \quad (52)$$

$$(\tilde{C}_i^A)^{NC} \rightarrow -\tilde{C}_i^A. \quad (53)$$

Similarly for the case of $D_{13}(1520)$ and $P_{13}(1720)$, the neutral current form factors \tilde{C}_i^V and \tilde{C}_i^A are given by:

$$(\tilde{C}_i^V)^{NC} \xrightarrow{\text{for p}} (1 - 2\sin^2\theta_W)C_i^p - \frac{1}{2}C_i^n \quad i = 3, 4, 5 \quad (54)$$

$$(\tilde{C}_i^V)^{NC} \xrightarrow{\text{for n}} (1 - 2\sin^2\theta_W)C_i^n - \frac{1}{2}C_i^p \quad i = 3, 4, 5 \quad (55)$$

$$(\tilde{C}_i^A)^{NC} \rightarrow \pm \frac{1}{2}\tilde{C}_i^A \quad i = 5 \quad (56)$$

where plus(minus) sign stands for proton(neutron) targets.

B. Spin $\frac{1}{2}$ resonances

For the neutral current process producing a spin $\frac{1}{2}$ resonance in the intermediate state, the hadronic current is given by Eq. 33. $\Gamma_{\frac{1}{2}}^\mu$ is the vertex function which for positive parity states is given by Eq. 34 and for negative parity states is given by Eq. 35. The vector and axial vector parts of the current are written in terms of vector and axial vector form factors and have the same form as given in Eqs. 36 and 37, but with a modified form factor corresponding to isospin $\frac{1}{2}$ resonance and a different expression for charged (\tilde{F}_i^p) and neutral (\tilde{F}_i^n) resonant states with the replacement of $F_{1,2}^{p,n}$ by $\tilde{F}_{1,2}^{p,n}$.

The explicit expressions for which are written as

$$\begin{aligned} \tilde{F}_i^p &= \left(\frac{1}{2} - 2\sin^2\theta_W\right)F_i^p - \frac{1}{2}F_i^n \\ \tilde{F}_A^p &= \frac{1}{2}F_A \end{aligned} \quad (57)$$

for the positive charged state and

$$\begin{aligned} \tilde{F}_i^n &= \left(\frac{1}{2} - 2\sin^2\theta_W\right)F_i^n - \frac{1}{2}F_i^p \\ \tilde{F}_A^n &= -\frac{1}{2}F_A \end{aligned} \quad (58)$$

for the negative charged state. F_i 's($i=1,2,A,P$) are defined in section-II B 1.

III. RESULTS AND DISCUSSION

In this section, we present the results of the numerical calculations and discuss the findings. The results are presented for the total scattering cross section by integrating over the kinematical variables in Eq.3, where the matrix element is given by Eq.4. In the expression of the matrix element, the leptonic current is given by Eq.5 and the hadronic current $j^{\mu(H)}$ is written as the sum of the contributions from the resonant terms including $\Delta(1232)$ resonance and non-resonant background(NRB) terms i.e.

$$j^{\mu(H)} = j_\Delta^\mu + j_{NRB}^\mu + j_R^\mu, \quad (59)$$

where

$$\begin{aligned} j_\Delta^\mu &= j_{s,\Delta}^\mu + j_{u,\Delta}^\mu \\ j_R^\mu &= j_{s,R}^\mu + j_{u,R}^\mu \end{aligned} \quad (60)$$

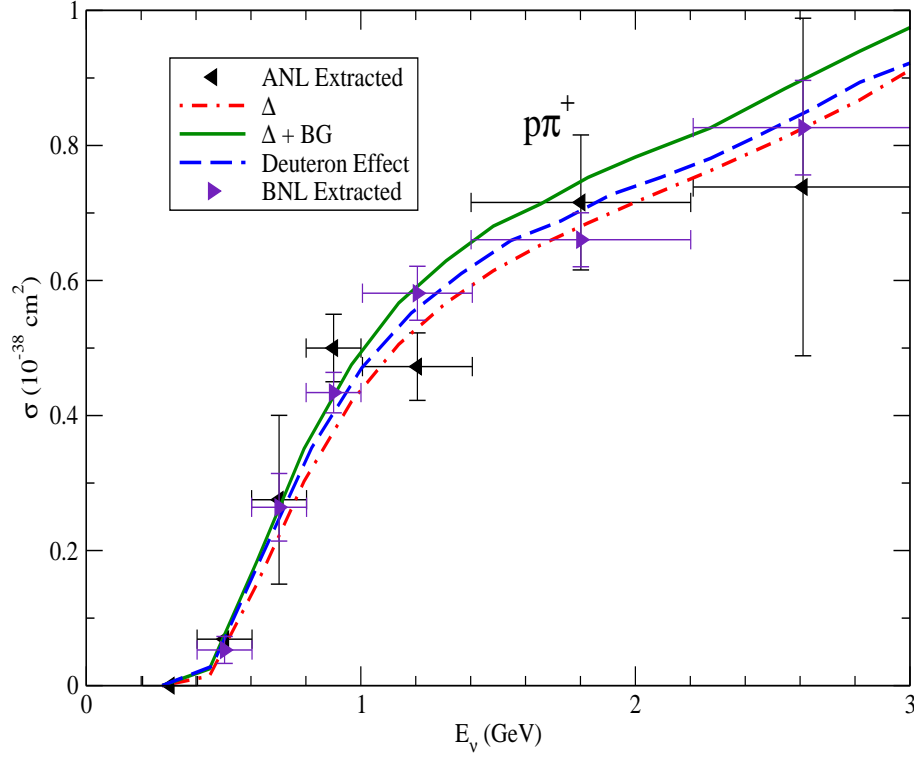


FIG. 6: Total scattering cross section for $\nu_\mu p \rightarrow \mu^- p \pi^+$ process. Experimental results are reanalyzed data points of ANL and BNL experiments by Wilkinson et al. [32]. No invariant mass cut has been applied. Dashed-dotted line is the result of the scattering cross section obtained by considering only the contribution from $\Delta(1232)$ resonance. When we also include non-resonant background terms in our calculations, the results are presented with solid line. The final results when deuteron effect is also taken into account has been shown by the long dashed line

and $j_{NRB}^{\mu,CC}$ for the charged current induced processes is

$$j_{NRB}^{\mu,CC} = j^\mu|_{NP} + j^\mu|_{CP} + j^\mu|_{CT} + j^\mu|_{PP} + j^\mu|_{PF}, \quad (61)$$

and for the neutral current induced processes is

$$j_{NRB}^{\mu,NC} = j^\mu|_{NP} + j^\mu|_{CP} \quad (62)$$

In Eq. 59, j_R^μ represents the contributions of all the higher resonances (other than $\Delta(1232)$) for the direct(s-channel) and cross(u-channel) terms wherever applicable:

$$j_R^\mu = j_{P_{11}(1440)}^\mu + j_{S_{11}(1535)}^\mu + j_{S_{11}(1650)}^\mu + j_{D_{13}(1520)}^\mu + j_{P_{13}(1720)}^\mu.$$

By $\Delta(1232)$ dominance we mean the contribution of s-channel as well as u-channel resonant terms (i.e. $= j_{s,\Delta}^\mu + j_{u,\Delta}^\mu$). $j_{NRB}^{\mu,CC}$ represents the hadronic current for charged current processes where the contributing terms are nucleon pole(NP), cross nucleon pole(CP), contact term(CT), pion pole(PP) and pion in flight(PF) terms. j_R^μ denotes the hadronic current for the other higher resonances, for which we have taken the contribution from s- as well as u- channels.

We must point out that in all the curves shown in the various figures, the places where we say $\Delta(1232)$ dominance means that the hadronic tensor $H^{\mu\nu}$ is obtained by evaluating $j_{s,\Delta}^{\mu\dagger} j_{s,\Delta}^\nu + j_{s,\Delta}^{\mu\dagger} j_{u,\Delta}^\nu + j_{u,\Delta}^{\mu\dagger} j_{s,\Delta}^\nu + j_{u,\Delta}^{\mu\dagger} j_{u,\Delta}^\nu$. When we say that the contributions from the background terms are also included, it is meant that the hadronic tensor has now the contribution from the square of $j_{NRB}^{\mu,CC}$ given in Eq. 61 and the terms arising due to the interference of j_Δ^μ and $j_{NRB}^{\mu,CC}$ as given in Eqs. 60 and 61, respectively. Finally, the results of full calculations would imply square of $j^\mu(H)$ given in Eq.59 to get the final expression for the hadronic tensor.

Furthermore, this is to be pointed out that the non-resonant background terms have been obtained using SU(2) non-linear sigma Lagrangian for pions and nucleons interaction. Due to the limitations of this model at higher energies [53], we have put a constraint on the center of mass energy(W) as $W_{min} = M + m_\pi$ and $W_{max} = 1.2 \text{ GeV}$

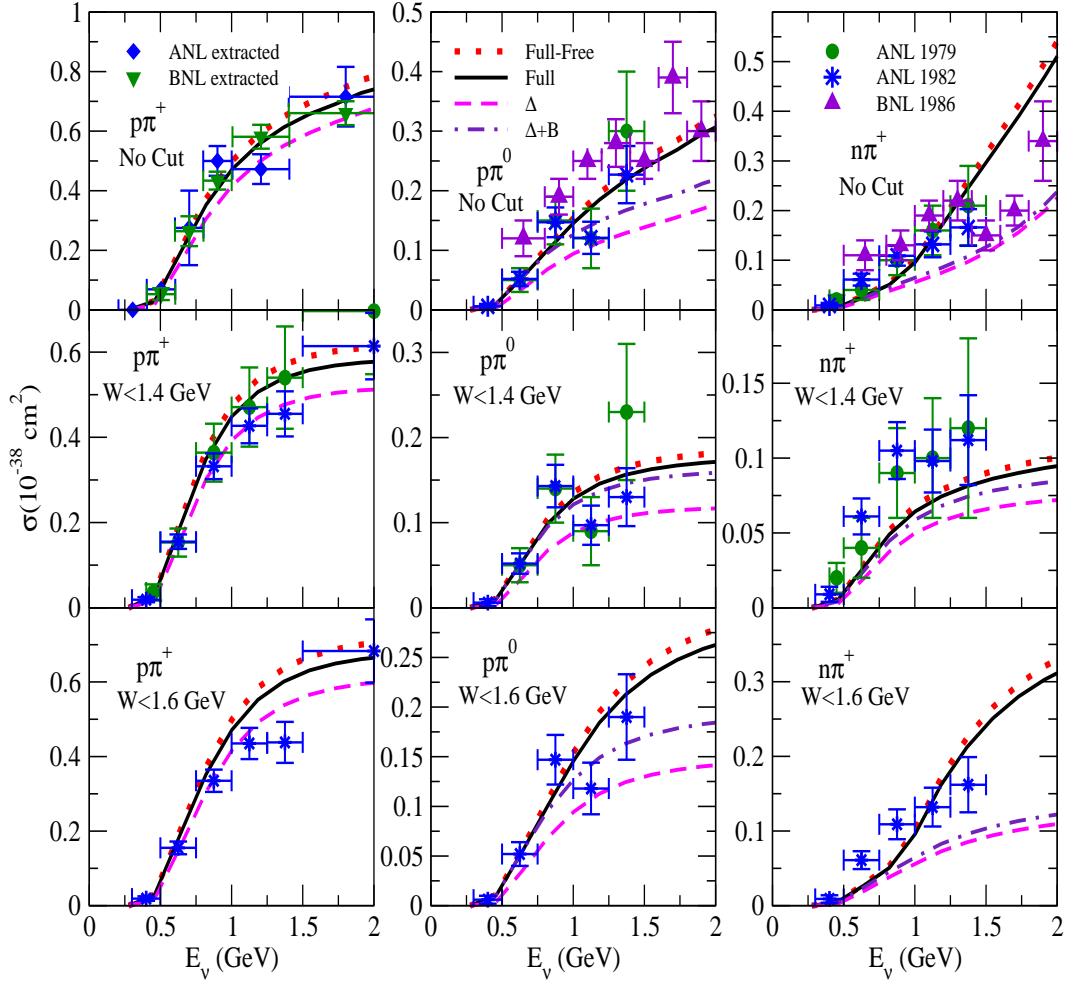


FIG. 7: Total scattering cross section for the charged current neutrino induced pion production processes: $\nu_\mu p \rightarrow \mu^- p \pi^+$ (Left panel), $\nu_\mu n \rightarrow \mu^- p \pi^0$ (Central panel), $\nu_\mu n \rightarrow \mu^- n \pi^+$ (Right panel). The dashed line is the result calculated in the $\Delta(1232)$ dominance model, dashed-dotted line is the result obtained when we include non-resonant background terms in our calculations. The solid line is the result of our full calculation when other resonances like $P_{11}(1440)$, $D_{13}(1520)$, $S_{11}(1535)$, $S_{11}(1650)$ and $P_{13}(1720)$ are also included. All the above three cases are with deuteron effect. The dotted line is the result of the full calculation without deuteron effect. The results in the top panels are obtained when we have not included any cut on invariant mass. The middle panel shows the results with a cut on center of mass energy of 1.4 GeV ($W < 1.4 \text{ GeV}$), while in the bottom panel a cut of $W < 1.6 \text{ GeV}$ is introduced while calculating total scattering cross section. Data points quoted as ANL extracted and BNL extracted are the reanalyzed data by Wilkinson et al. [32]. Other data points in figures are the results from ANL [28] and BNL [29] experiments.

while evaluating the non-resonant background terms. We have varied $C_5^A(0)$ and axial mass M_A in $C_5^A(Q^2)$ to get the best description for the reanalyzed data [32] of ANL and BNL experiments in the case of $\nu_\mu p \rightarrow \mu^- p \pi^+$ process. This constraint on W (i.e. $M + m_\pi \leq W \leq 1.2 \text{ GeV}$) has been put in all numerical evaluations while considering non-resonant background contribution.

Since earlier experiments to measure charged current neutrino induced single pion production were mainly performed using hydrogen/deuteron target like the experiments at ANL [28] and BNL [29], therefore, deuteron correction factor must be taken into account. In a recent analysis by Wilkinson et al. [32] experimental results of ANL [28] and BNL [29] have been normalized to deuteron data. Therefore, we have taken deuteron effect by following the prescription of Hernandez et al. [81] and write

$$\left(\frac{d\sigma}{dQ^2 dW} \right)_{\nu d} = \int d\mathbf{p}_p^d |\Psi_d(\mathbf{p}_p^d)|^2 \frac{M}{E_p^d} \left(\frac{d\sigma}{dQ^2 dW} \right)_{\text{off shell}}, \quad (63)$$

where the four momentum of the proton inside the deuteron is described by $p^\mu = (E_p^d, \mathbf{p}_p^d)$ with $E_p^d (= M_{\text{Deuteron}} -$

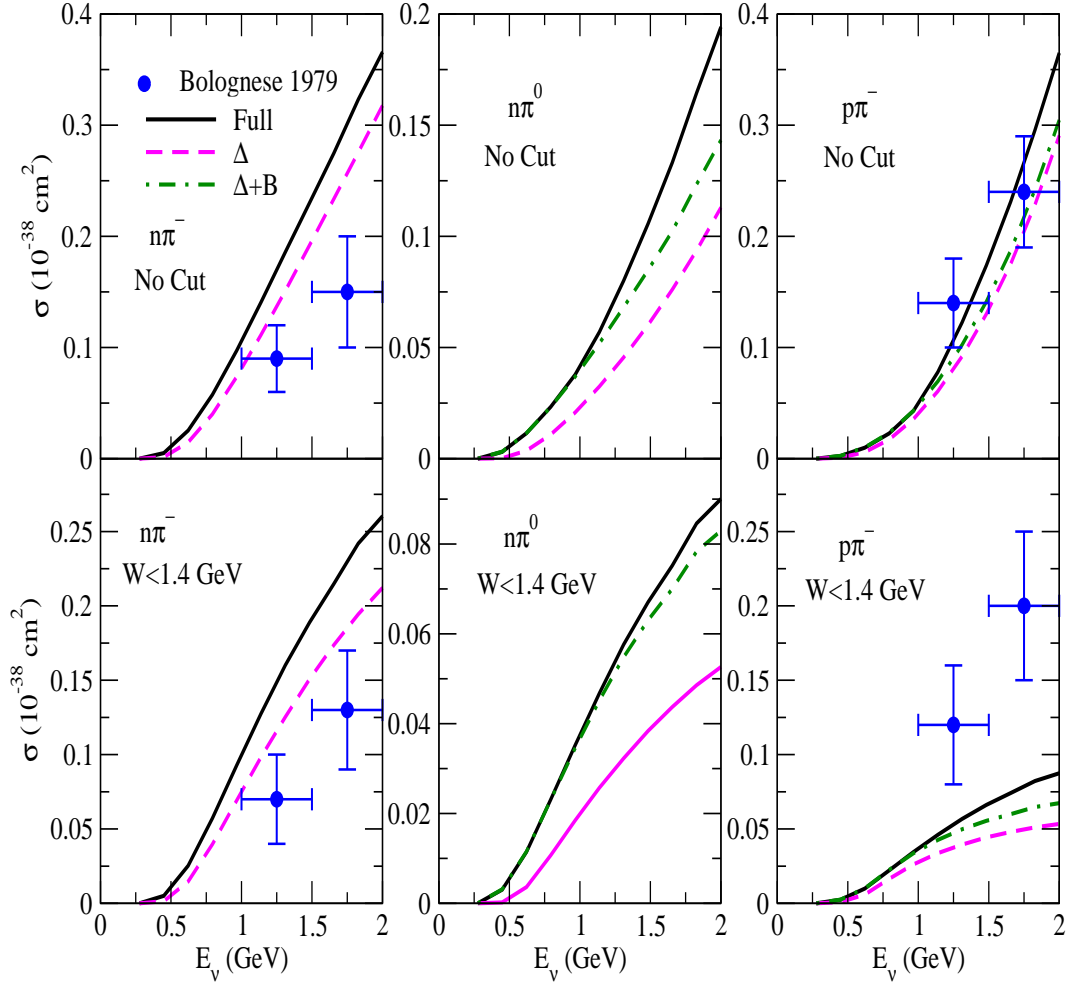


FIG. 8: Total scattering cross section for the charged current antineutrino induced pion production processes with deuteron effect. The results presented on the left panel are for $\bar{\nu}_\mu n \rightarrow \mu^+ n \pi^-$, on the central panel are for $\bar{\nu}_\mu n \rightarrow \mu^+ n \pi^0$, and on the right panel are for $\bar{\nu}_\mu p \rightarrow \mu^+ p \pi^-$ processes. Data points are the experimental results from Ref.[64]. The theoretical results presented here should be corrected for the nuclear medium effects before making any comparison with the experimental data. Lines have the same meaning as in Fig.7.

$\sqrt{M^2 + |\mathbf{p}_p^d|^2}$) as the energy of the off shell proton inside the deuteron and M_{Deuteron} is the deuteron mass. $\left(\frac{d\sigma}{dQ^2 dW}\right)_{\text{off shell}}$ is obtained by using Eq.3. In the above expression $|\Psi_d|^2 = |\Psi_0|^2 + |\Psi_2|^2$, where Ψ_0 and Ψ_2 are the deuteron wave functions for the S-state and D-state, respectively and have been taken from the works of Lacombe et al. [82].

In Fig. 6, we have shown the results for the total scattering cross section for the charged current neutrino induced $1\pi^+$ production process on proton target i.e. for the reaction $\nu_\mu p \rightarrow \mu^- p \pi^+$. In these calculations no invariant mass cut has been applied. The results are presented for the total scattering cross section in $\Delta(1232)$ - dominance model, then we include the contributions from the non-resonant background(NRB) terms. It may be pointed out that in the case of $1\pi^+$ production process on proton target there is no contribution from the higher resonances considered here other than $\Delta(1232)$ resonance. The final results are with deuteron effect which has been obtained by using Eq. 63. It may be observed that the inclusion of deuteron effect results into an overall reduction of $\sim 4 - 6\%$ in the total scattering cross section. The present results are compared with the reanalyzed experimental analysis of ANL [28] and BNL [29] data by Wilkinson et al. [32]. We found the best fit of the total scattering cross section $\sigma(\nu_\mu p \rightarrow \mu^- p \pi^+)$ when $C_5^A(0) = 1.0$ and $M_A = 1.026$ GeV are used in the expression.

We have also calculated total scattering cross section for the charged current neutrino induced pion production processes and the results are presented in Fig. 7. The experimental points for $\pi^+ p$ channel is the reanalyzed data by Wilkinson et al. [32] of the ANL [28] and BNL [29] experiments. While for the other channels like $\pi^0 p$ and $\pi^+ n$ the

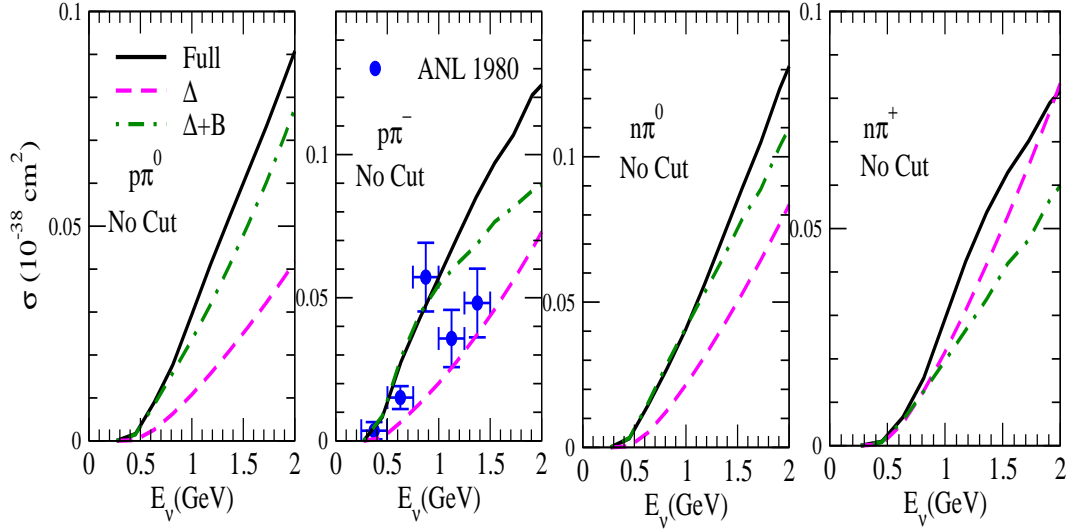


FIG. 9: Total scattering cross section for neutral current neutrino induced pion production processes with deuteron effect. The results presented from the left to the right panels are for $\nu p \rightarrow \nu p \pi^0$, $\nu n \rightarrow \nu p \pi^-$, $\nu n \rightarrow \nu n \pi^0$, and $\nu p \rightarrow \nu n \pi^+$ processes. Data points are the experimental results from ANL [65] experiment. Results are obtained without using any cut on the invariant mass W . Lines have the same meaning as in Fig.7.

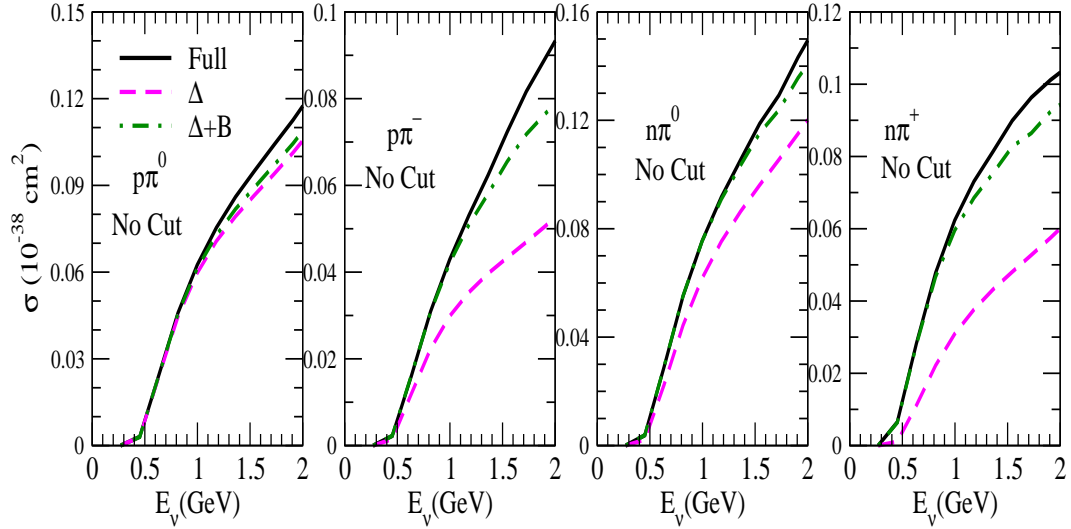


FIG. 10: Total scattering cross section for neutral current antineutrino induced pion production processes with deuteron effect. The results presented from the left to the right panels are for $\bar{\nu} p \rightarrow \bar{\nu} p \pi^0$, $\bar{\nu} n \rightarrow \bar{\nu} p \pi^-$, $\bar{\nu} n \rightarrow \bar{\nu} n \pi^0$, and $\bar{\nu} p \rightarrow \bar{\nu} n \pi^+$ processes. Results are obtained without using any cut on the invariant mass W . Lines have the same meaning as in Fig.7.

data are of ANL [28] and BNL [29] experiments. In the case of $\nu_\mu p \rightarrow \mu^- p \pi^+$ induced reaction, the main contribution to the total scattering cross section comes from the $\Delta(1232)$ resonance and there is no contribution from the higher resonances which are considered here. We find that due to the presence of the non-resonant background terms there is an increase in the cross section which is about 12% at $E_{\nu_\mu}=1\text{GeV}$ which becomes $\sim 8\%$ at $E_{\nu_\mu}=2\text{GeV}$.

For $\nu_\mu n \rightarrow \mu^- n \pi^+$ as well as $\nu_\mu n \rightarrow \mu^- p \pi^0$ processes, there are contributions from the non-resonant background terms as well as other higher resonant terms besides the $\Delta(1232)$ - dominance. The net contribution to the total pion production due to the presence of the non-resonant background terms in $\nu_\mu n \rightarrow \mu^- n \pi^+$ reaction results in an increase in the cross section of about 12% at $E_{\nu_\mu}=1\text{GeV}$ which becomes 6% at $E_{\nu_\mu}=2\text{GeV}$. When other higher resonances are also taken into account there is a further increase in the cross section by about 40% at $E_{\nu_\mu}=1\text{GeV}$ which becomes 55% at $E_{\nu_\mu}=2\text{GeV}$. While in the case of $\nu_\mu n \rightarrow \mu^- p \pi^0$ due to the presence of the background terms the total increase is about 26% at $E_{\nu_\mu}=1\text{GeV}$ and 18% at $E_{\nu_\mu}=2\text{GeV}$. Due to the presence of other higher resonances there is a further increase of about 35% at $E_{\nu_\mu}=1\text{GeV}$ and 40% at $E_{\nu_\mu}=2\text{GeV}$. Thus, we find that the inclusion of higher resonant terms

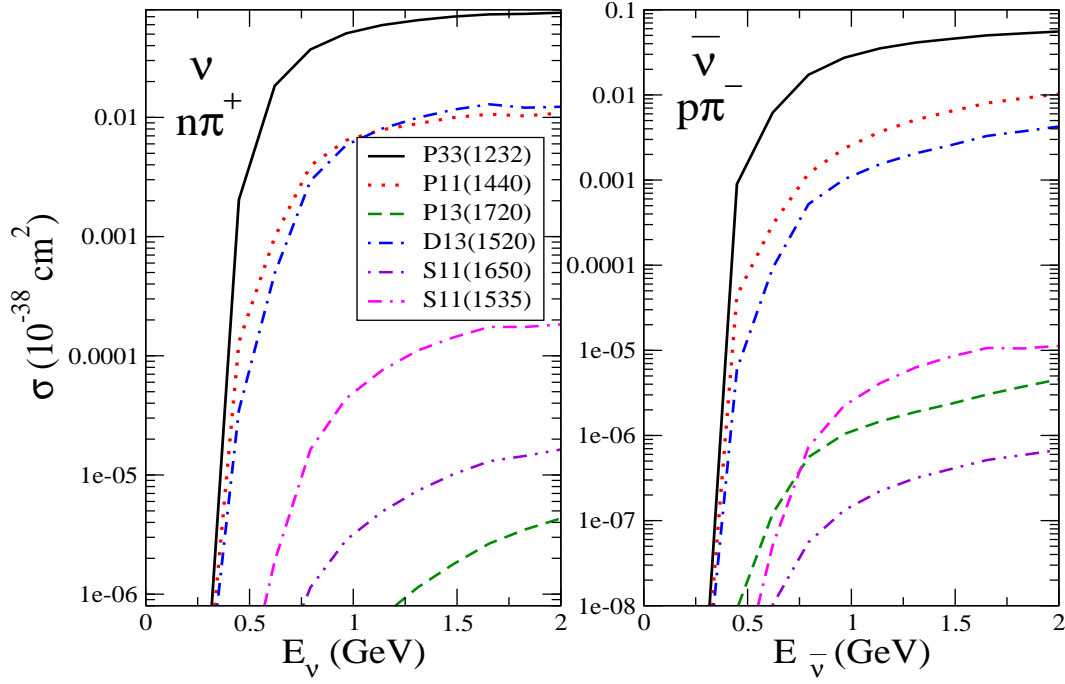


FIG. 11: The results are presented for the total scattering cross section for $\nu_\mu n \rightarrow \mu^- n \pi^+$ (Left panel) and $\bar{\nu}_\mu p \rightarrow \mu^+ p \pi^-$ (Right panel) processes where the individual contribution of various resonances have been shown.

lead to a significant increase in the cross section for $\nu_\mu n \rightarrow \mu^- n \pi^+$ and $\nu_\mu n \rightarrow \mu^- p \pi^0$ processes. Furthermore, it may also be concluded from the above observations that contribution from non-resonant background terms decreases with the increase in neutrino energy, while the total scattering cross section increases when we also include other higher resonances in our calculations.

When a cut of $W \leq 1.4 \text{ GeV}$ or $W \leq 1.6 \text{ GeV}$ on the center of mass energy is applied then due to the presence of the non-resonant background terms, the increase in the total scattering cross section at $E_{\nu_\mu} = 1 \text{ GeV}$ for $\nu_\mu p \rightarrow \mu^- p \pi^+$ is about 10%. For $\nu_\mu n \rightarrow \mu^- n \pi^+$ reaction this increase in the cross section is about 14% at $E_{\nu_\mu} = 1 \text{ GeV}$ which becomes 5% at $E_{\nu_\mu} = 2 \text{ GeV}$. When other higher resonances are also taken into account there is a further increase in the cross section which is about 40% at $E_{\nu_\mu} = 1 \text{ GeV}$. However, some energy dependence is observed and at $E_{\nu_\mu} = 2 \text{ GeV}$ this increase is $\sim 55\%$ for $W \leq 1.4 \text{ GeV}$ and $\sim 65\%$ for $W \leq 1.6 \text{ GeV}$. While in the case of $\nu_\mu n \rightarrow \mu^- p \pi^0$ due to the presence of the non-resonant background terms the total increase in cross section is about 27% at $E_{\nu_\mu} = 1 \text{ GeV}$ for $W \leq 1.4 \text{ GeV}$ or $W \leq 1.6 \text{ GeV}$. Due to the presence of other resonances there is a further increase of about 10% at $E_{\nu_\mu} = 1 \text{ GeV}$.

In Fig. 8, we have shown the results for the charged current antineutrino induced pion production processes. These results are presented in the $\Delta(1232)$ dominance model, including non-resonant background terms as well as with our full prescription given in Eq. 63. Here also in the case of $\bar{\nu}_\mu n \rightarrow \mu^+ n \pi^-$ reaction there is no contribution from the higher resonances other than $\Delta(1232)$ resonance. The inclusion of non-resonant background terms increases the cross section by around 24% at $E_{\nu_\mu} = 1 \text{ GeV}$ which becomes around 12% at $E_{\nu_\mu} = 2 \text{ GeV}$. For $\bar{\nu}_\mu p \rightarrow \mu^+ n \pi^0$ reaction, inclusion of non-resonant background terms increases cross section by around 42% at $E_{\nu_\mu} = 1 \text{ GeV}$ which becomes 20% at $E_{\nu_\mu} = 2 \text{ GeV}$. When other higher resonances are included, the cross section further increases by $\sim 45\%$ at $E_{\nu_\mu} = 1 \text{ GeV}$ which becomes 40% at $E_{\nu_\mu} = 2 \text{ GeV}$. In the case of $\bar{\nu}_\mu p \rightarrow \mu^+ p \pi^-$ reaction, when we perform calculations by including non-resonant background terms then cross section gets enhanced by around 16% at $E_{\nu_\mu} = 1 \text{ GeV}$ which becomes 4% at $E_{\nu_\mu} = 2 \text{ GeV}$. When other higher resonances are also included along with non-resonant background terms then cross section further increases by around 18% at $E_{\nu_\mu} = 1 \text{ GeV}$ and $\sim 20\%$ at $E_{\nu_\mu} = 2 \text{ GeV}$.

We have compared the present results with the experimental data of Gargamelle experiment performed at CERN PS where propane was used as the nuclear target. Since propane is a composite target therefore the cross sections would get modulated due to nuclear medium effects. Thus, the theoretical results presented in Fig. 8 should be corrected for the nuclear medium effects before making any comparison with the experimental data. We would like to point out that, in our earlier works [49, 50, 66] of charged and neutral current pion production in the $\Delta(1232)$ dominance model, we have observed that nuclear medium effect reduces the cross section significantly when the calculations are performed for nuclear targets and this helps in explaining the experimental data.

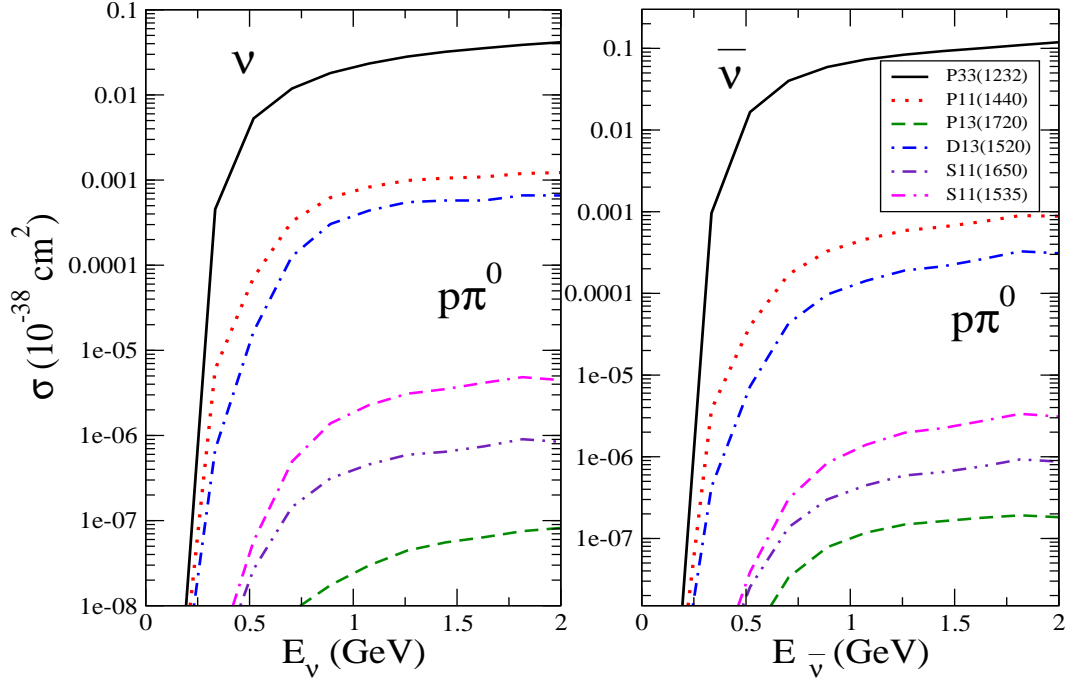


FIG. 12: The results are presented for the total scattering cross section for $\nu_\mu p \rightarrow \nu_\mu p \pi^0$ (Left panel) and $\bar{\nu}_\mu p \rightarrow \bar{\nu}_\mu p \pi^0$ (Right panel) processes where the individual contribution of various resonances have been shown.

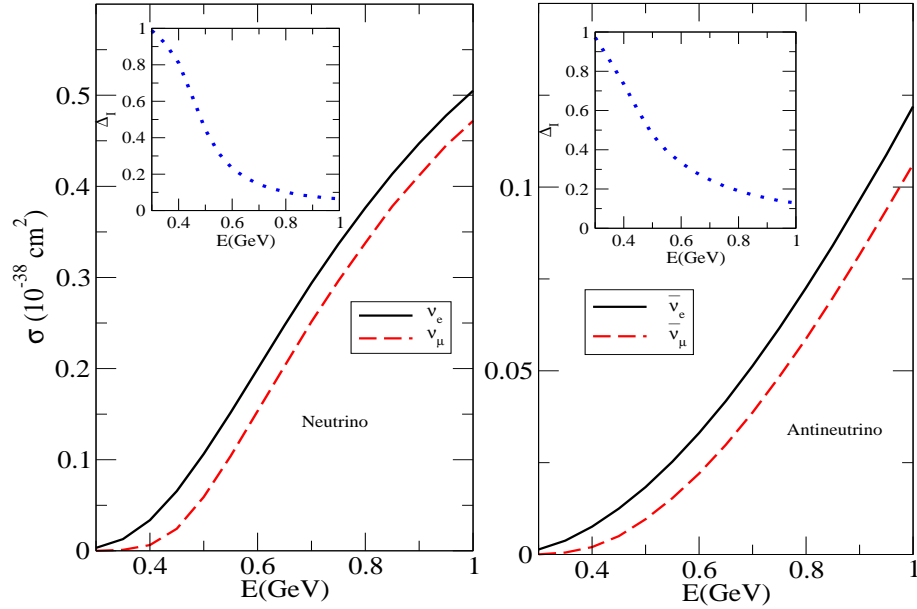


FIG. 13: Total scattering cross section for $\nu_l p \rightarrow l^- p \pi^+$ and $\bar{\nu}_l n \rightarrow l^+ n \pi^-$ processes with deuteron effect where $l = e$ (solid line), μ (dashed line). In the inset the results for $\Delta_I = \frac{\sigma_{\nu_e(\bar{\nu}_e)} - \sigma_{\nu_\mu(\bar{\nu}_\mu)}}{\sigma_{\nu_e(\bar{\nu}_e)}}$ for neutrino (left panel) and antineutrino (right panel) induced processes have been shown.

In Fig. 9 (Fig. 10), we have plotted the total scattering cross section for neutral current neutrino (antineutrino) induced pion production processes on proton and neutron targets. The experimental points are the data from ANL experiment [65]. Here also it may be observed that besides $\Delta(1232)$ resonant term, there is significant contribution from non-resonant background terms which results in an increase in the total scattering cross section in all the channels. Specifically, the increase in the cross section at $E_\nu = 1\text{GeV}$ due to non-resonant background terms in neutrino induced processes is $\sim 45\%$ for $\nu p \rightarrow \nu n \pi^+$, $\sim 15\%$ for $\nu p \rightarrow \nu p \pi^0$, $\sim 82\%$ for $\nu n \rightarrow \nu p \pi^-$ and $\sim 48\%$ for

$\nu n \rightarrow \nu n \pi^0$. Similarly, in the case of antineutrino induced processes the enhancement in the cross section due to the presence of non-resonant background terms is $\sim 4\%$ for $\bar{\nu} p \rightarrow \bar{\nu} p \pi^0$, $\sim 49\%$ for $\bar{\nu} p \rightarrow \bar{\nu} n \pi^+$, $\sim 18\%$ for $\bar{\nu} n \rightarrow \bar{\nu} n \pi^0$ and $\sim 30\%$ for $\bar{\nu} n \rightarrow \bar{\nu} p \pi^-$. We also observe that when higher resonant terms are included, there is no appreciable change in the cross sections which is in contrast to the observations made in the charged current induced reactions. For example, at $E_{\nu, \bar{\nu}} = 1\text{GeV}$ this increase is almost negligible for all the antineutrino induced processes on proton and neutron targets as well as neutrino induced processes on neutron target. There is $\sim 15\%$ enhancement in the cross sections in $\nu p \rightarrow \nu \pi^+ n$ and $\nu p \rightarrow \nu \pi^- p$ processes when higher resonant terms are included.

To explicitly show the contribution of individual resonances to the total scattering cross section, in Fig. 11, we have presented the results for $\nu_\mu n \rightarrow \mu^- n \pi^+$ and $\bar{\nu}_\mu p \rightarrow \mu^+ p \pi^-$ processes. It may be observed that the dominant contribution comes from $\Delta(1232)$ resonance followed by $P_{11}(1440)$ and $D_{13}(1520)$ resonances. However, the contribution for neutrino and antineutrino induced processes are not alike, for example, larger $\Delta(1232)$ dominance may be observed in the neutrino case than in the case of antineutrino induced processes. For the case of neutrino induced charged current processes, at $E_\nu = 1\text{GeV}$, the contribution to the total scattering cross section from $P_{11}(1440)$ ($D_{13}(1520)$) resonance is around 10% (12%) as that of the contribution from $\Delta(1232)$ resonance. However, at $E_\nu = 2\text{GeV}$ contribution of $P_{11}(1440)$ ($D_{13}(1520)$) resonance is around 14% (16%). For antineutrino induced charged current processes, at $E_{\bar{\nu}} = 1\text{GeV}$, the contribution to the total scattering cross section from $P_{11}(1440)$ ($D_{13}(1520)$) resonance is around 8% (2%) which becomes around 18% (6%) at $E_{\bar{\nu}} = 2\text{GeV}$ as that of the contribution from $\Delta(1232)$ resonance.

Similar study has also been made for the (anti)neutrino induced neutral current processes. To explicitly show the contributions of different resonant terms, in Fig. 12, we have presented the results for $\nu p \rightarrow \nu p \pi^0$ and $\bar{\nu} p \rightarrow \bar{\nu} p \pi^0$ reactions. In this case it may be observed that the dominant contribution is still from $\Delta(1232)$ resonance followed by $P_{11}(1440)$ and $D_{13}(1520)$ resonances. However, a larger $\Delta(1232)$ dominance is observed for antineutrino induced processes as compared to neutrino induced reaction, which is in contrast to the observation in the case of charged current induced processes. For example, for the case of neutrino induced neutral current processes, the contribution to the total scattering cross section from $P_{11}(1440)$ resonance is 3% as that of the contribution from $\Delta(1232)$ resonance in the energy range $E_\nu = 1 - 2\text{GeV}$. However, the contribution from $D_{13}(1520)$ resonance in the energy range $E_\nu = 1 - 2\text{GeV}$ is around 2% . For antineutrino induced charged current processes, in the energy range $E_{\bar{\nu}} = 1 - 2\text{GeV}$, the contribution to the total scattering cross section from $P_{11}(1440)$ ($D_{13}(1520)$) resonance is almost negligible to that of the contribution from $\Delta(1232)$ resonance.

In Fig. 13, we have shown the lepton mass effect for the $\nu_e(\nu_\mu)$ and $\bar{\nu}_e(\bar{\nu}_\mu)$ induced processes by considering the reactions $\nu_l p \rightarrow l^- p \pi^+$ and $\bar{\nu}_l n \rightarrow l^+ n \pi^-$. In the inset of these figures we have also shown the fractional change in the cross sections $\Delta_I = \frac{\sigma_{\nu_e(\bar{\nu}_e)} - \sigma_{\nu_\mu(\bar{\nu}_\mu)}}{\sigma_{\nu_e(\bar{\nu}_e)}}$ for neutrino(left panel) and antineutrino(right panel) induced processes. These results are shown up to $E_{\nu(\bar{\nu})} \leq 1\text{GeV}$. As may be observed from these curves that there is significant effect of lepton mass(electron vs muon) on the total scattering cross section. This study may be helpful in the analysis of data of the experiments planned in the $\sim 1\text{GeV}$ energy region looking for the signals of CP violation in the leptonic sector.

IV. CONCLUSIONS

In this work, we have presented a study of weak charged and neutral current induced single pion production from nucleons. The results have been presented for the total scattering cross sections by including the contributions of $P_{33}(1232)$, $P_{11}(1440)$, $S_{11}(1535)$, $D_{13}(1520)$, $S_{11}(1650)$ and $P_{13}(1720)$ resonances and the non-resonant background terms. Resonant terms are obtained using phenomenological Lagrangian while non-resonant background terms have been obtained using a SU(2) non-linear sigma model for pion-nucleon interaction Lagrangian.

We find that:

1. The pions are produced predominantly through $P_{33}(1232)$ resonance formation in $\nu_\mu p \rightarrow \mu^- p \pi^+$ channel. The best description of the reanalyzed experimental data of ANL and BNL experiments by Wilkinson et al. [32] for this channel is obtained when we take $C_5^A(0)=1.0$ and $M_A=1.026\text{GeV}$ for N- Δ axial vector transition current form factor $C_5^A(Q^2)$.
2. The enhancement in the cross section due to the presence of non-resonant background terms at $E_\nu = 1(2)\text{ GeV}$ is around $12(8)\%$ for $\nu_\mu p \rightarrow \mu^- p \pi^+$ process, and $24(12)\%$ for $\bar{\nu}_\mu n \rightarrow \mu^+ n \pi^-$ process. It may be noted that the energy dependence of non-resonant contributions in neutrino vs antineutrino induced processes is different. Higher resonances considered in this work do not contribute to these channels.
3. For $\nu_\mu n \rightarrow \mu^- p \pi^0$ process, we find the enhancement in cross section to be around 26% at $E_\nu = 1\text{GeV}$ when non-resonant background terms are included. There is a further increase of $\sim 9\%$ in the cross section when higher resonances are taken into account. The non-resonant contributions in the case of $\nu_\mu n \rightarrow \mu^- n \pi^+$ process

is around 14% which becomes 42% when higher resonances are also included. The ratio of the cross sections for $\nu_\mu n \rightarrow \mu^- p \pi^0$ to $\nu_\mu n \rightarrow \mu^- n \pi^+$ processes is found to be ~ 1.7 when evaluated in the $\Delta(1232)$ dominance model, which becomes ~ 2 if non-resonant background terms are included, and 1.5 when other higher resonances are also taken into account.

4. In the case of $\bar{\nu}_\mu p \rightarrow \mu^+ n \pi^0$ process the enhancement in the cross section due to the presence of non-resonant background terms is $\sim 42\%$ at $E_\nu = 1$ GeV, which in the case of $\bar{\nu}_\mu p \rightarrow \mu^+ p \pi^-$ process is $\sim 16\%$. The contribution of higher resonance terms is quite small ($\sim 3\%$) in both the channels. The ratio of the cross sections for the processes $\bar{\nu}_\mu p \rightarrow \mu^+ n \pi^0$ and $\bar{\nu}_\mu p \rightarrow \mu^+ p \pi^-$ is found to be ~ 0.6 when evaluated in the $\Delta(1232)$ dominance model which becomes ~ 0.8 if non-resonant background terms are also included.
5. Qualitatively, the results for the neutral current induced pion production processes are similar to the charged ones, however, quantitatively there are differences in the relative contribution of various terms.
 - (i) The contribution of non-resonant terms leads to an increase in cross section for all the channels involving proton as well as neutron targets. The maximum contribution due to non-resonant terms is for $\nu n \rightarrow \nu p \pi^-$ process and the minimum contribution is for $\bar{\nu} p \rightarrow \bar{\nu} p \pi^0$.
 - (ii) When higher resonant terms are included, there is no appreciable change in the cross sections which is in contrast to the observations made in the charged current induced reactions. At $E_{\nu, \bar{\nu}} = 1$ GeV this increase is almost negligible for all the antineutrino induced processes on proton and neutron targets as well as neutrino induced processes on neutron target. In the case of other neutrino induced processes like $\nu p \rightarrow \nu \pi^+ n$ and $\nu p \rightarrow \nu \pi^- p$ this increase in cross section due to the inclusion of higher resonant terms is about 15%.

These results may be used as a benchmark calculations for weak charged and neutral current induced one pion production processes from nucleons. The present model can be applied to study the pion production from nuclear targets. This work is presently going on and will be reported elsewhere.

V. ACKNOWLEDGMENTS

M. S. A. is thankful to Department of Science and Technology(DST), Government of India for providing financial assistance under Grant No. SR/S2/HEP-18/2012. M. R. A. and S. C. are thankful to University Grant Commission for providing financial assistance under UGC - Start up grant(No. F.30-90/2015(BSR)).

-
- [1] A. A. Aguilar-Arevalo *et al.* [MiniBooNE Collaboration], Phys. Rev. D **81**, 013005 (2010).
 - [2] A. A. Aguilar-Arevalo *et al.* [MiniBooNE Collaboration], Phys. Rev. D **83**, 052007 (2011).
 - [3] A. A. Aguilar-Arevalo *et al.* [MiniBooNE Collaboration], Phys. Rev. D **83**, 052009 (2011).
 - [4] T. Katori [MiniBooNE and SciBooNE Collaborations], AIP Conf. Proc. **1663**, 020001 (2015).
 - [5] K. Abe *et al.* [T2K Collaboration], PTEP **2015**, no. 4, 043C01 (2015).
 - [6] K. Abe *et al.* [T2K Collaboration], Phys. Rev. D **88**, 032002 (2013).
 - [7] F. Jedin [NOvA Collaboration], J. Phys. Conf. Ser. **490**, 012019 (2014).
 - [8] H. Chen *et al.* [MicroBooNE Collaboration], FERMILAB-PROPOSAL-0974.
 - [9] R. Acciarri *et al.* [ArgoNeuT Collaboration], Phys. Rev. Lett. **113**, 261801 (2014) [Erratum-ibid. **114**, 039901 (2015)].
 - [10] J. B. Spitz, "Measuring Muon-Neutrino Charged-Current Differential Cross Sections with a Liquid Argon Time Projection Chamber," FERMILAB-THESIS-2011-36.
 - [11] T. Patzak [LAGUNA-LBNO Collaboration], Nucl. Instrum. Meth. A **695**, 184 (2012).
 - [12] R. Saakian [MINOS Collaboration], Phys. Atom. Nucl. **67**, 1084 (2004) [Yad. Fiz. **67**, 1112 (2004)].
 - [13] www.dunescience.org
 - [14] O. Benhar, P. Huber, C. Mariani and D. Meloni, arXiv:1501.06448 [nucl-th].
 - [15] L. Alvarez-Ruso, Y. Hayato and J. Nieves, New J. Phys. **16**, 075015 (2014).
 - [16] H. Gallagher, G. Garvey and G. P. Zeller, Ann. Rev. Nucl. Part. Sci. **61**, 355 (2011).
 - [17] J. G. Morfin, J. Nieves and J. T. Sobczyk, Adv. High Energy Phys. **2012**, 934597 (2012).
 - [18] J. A. Formaggio and G. P. Zeller, Rev. Mod. Phys. **84**, 1307 (2012).
 - [19] R. Gran [K2K Collaboration], Nucl. Phys. Proc. Suppl. **221**, 98 (2011).
 - [20] C. Mariani [K2K Collaboration], AIP Conf. Proc. **1189**, 339 (2009).
 - [21] C. Mariani *et al.* [K2K Collaboration], Phys. Rev. D **83**, 054023 (2011).
 - [22] L. Whitehead [K2K Collaboration], PoS NFACT **08**, 064 (2008).
 - [23] B. Eberly *et al.* [MINERvA Collaboration], arXiv:1406.6415 [hep-ex].
 - [24] G. A. Fiorentini *et al.* [MINERvA Collaboration], Phys. Rev. Lett. **111**, 022502 (2013).

- [25] L. Fields *et al.* [MINERvA Collaboration], Phys. Rev. Lett. **111**, 022501 (2013)
- [26] T. Walton *et al.* [MINERvA Collaboration], Phys. Rev. D **91**, no. 7, 071301 (2015).
- [27] B. G. Tice *et al.* [MINERvA Collaboration], Phys. Rev. Lett. **112**, 231801 (2014).
- [28] G. M. Radecky *et al.*, Phys. Rev. D **25**, 1161 (1982) [Erratum-ibid. D **26**, 3297 (1982)], S. J. Barish *et al.*, Phys. Rev. D **16**, 3103 (1977); Phys. Rev. D **19**, 2521 (1979).
- [29] T. Kitagaki *et al.*, Phys. Rev. D **34**, 2554 (1986); Phys. Rev. D **42**, 1331 (1990).
- [30] K. M. Graczyk *et al.*, Phys. Rev. D **80**, 093001 (2009).
- [31] K. M. Graczyk, J. Żmuda and J. T. Sobczyk, Phys. Rev. D **90**, 093001 (2014).
- [32] C. Wilkinson *et al.*, Phys. Rev. D **90**, 112017 (2014).
- [33] S. M. Berman and M. J. G. Veltman, Nuovo Cim. **38**, 993 (1965).
- [34] J. S. Bell and S. M. Berman, Nuovo Cim. **25**, 404 (1962).
- [35] J. S. Bell and C. H. Llewellyn Smith, Nucl. Phys. B **24**, 285 (1970).
- [36] C. H. Albright and L. S. Liu, Phys. Rev. Lett. **13**, 673 (1964).
- [37] C. H. Albright and L. S. Liu, Phys. Rev. Lett. **14**, 324 (1965).
- [38] C. H. Albright and L. S. Liu, Phys. Rev. **140**, B748 (1965).
- [39] C. H. Llewellyn Smith, Phys. Rept. **3**, 261 (1972).
- [40] P. A. Schreiner and F. Von Hippel, Nucl. Phys. B **58**, 333 (1973).
- [41] F. Ravndal, Lett. Nuovo Cim. **3S2**, 631 (1972) [Lett. Nuovo Cim. **3**, 631 (1972)].
- [42] D. Rein and L. M. Sehgal, Annals Phys. **133**, 79 (1981).
- [43] K. S. Kuzmin, V. V. Lyubushkin and V. A. Naumov, Mod. Phys. Lett. A **19**, 2815 (2004) [Phys. Part. Nucl. **35**, S133 (2004)].
- [44] K. S. Kuzmin, V. V. Lyubushkin and V. A. Naumov, Nucl. Phys. Proc. Suppl. **139**, 158 (2005).
- [45] J. J. Wu and B. S. Zou, Few-Body Systems, **1** (2015).
- [46] T. Sato, D. Uno and T. S. H. Lee, Phys. Rev. C **67**, 065201 (2003).
- [47] J. J. Wu, T. Sato and T.-S. H. Lee, Phys. Rev. C **91**, no. 3, 035203 (2015).
- [48] H. Kamano, S. X. Nakamura, T.-S. H. Lee and T. Sato, Phys. Rev. C **88**, no. 3, 035209 (2013).
- [49] M. Sajjad Athar, S. Chauhan and S. K. Singh, J. Phys. G **37**, 015005 (2010).
- [50] M. Sajjad Athar, S. Chauhan and S. K. Singh, Eur. Phys. J. A **43**, 209 (2010).
- [51] M. Sajjad Athar, S. Ahmad and S. K. Singh, Eur. Phys. J. A **24**, 459 (2005).
- [52] T. Leitner, L. Alvarez-Ruso and U. Mosel, Phys. Rev. C **73**, 065502 (2006).
- [53] E. Hernandez, J. Nieves and M. Valverde, Phys. Rev. D **76**, 033005 (2007).
- [54] O. Lalakulich, T. Leitner, O. Buss and U. Mosel, Phys. Rev. D **82**, 093001 (2010).
- [55] G. L. Fogli and G. Nardulli, Nucl. Phys. B **160**, 116 (1979).
- [56] G. L. Fogli and G. Nardulli, Nucl. Phys. B **165**, 162 (1980).
- [57] W. Y. Lee *et al.*, Phys. Rev. Lett. **38**, 202 (1977).
- [58] J. Bell *et al.*, Phys. Rev. Lett. **41**, 1008 (1978).
- [59] P. Allen *et al.* [Aachen-Bonn-CERN-Munich-Oxford Collaboration], Nucl. Phys. B **176**, 269 (1980).
- [60] X. Zhang and B. D. Serot, Phys. Rev. C **86**, 035502 (2012).
- [61] O. Lalakulich and U. Mosel, Phys. Rev. C **87**, 014602 (2013).
- [62] O. Lalakulich and U. Mosel, Phys. Rev. C **88**, 017601 (2013).
- [63] T. Leitner *et al.*, Phys. Rev. C **79**, 034601 (2009).
- [64] T. Bolognese *et al.*, Phys. Lett. B **81**, 393 (1979).
- [65] M. Derrick *et al.*, Phys. Lett. B **92**, 363 (1980).
- [66] S. Ahmad, M. Sajjad Athar and S. K. Singh, Phys. Rev. D **74**, 073008 (2006).
- [67] S. Galster *et al.*, Nucl. Phys. B **32**, 221 (1971).
- [68] V. Bernard, L. Elouadrhiri and U. G. Meissner, J. Phys. G **28**, R1 (2002).
- [69] O. Lalakulich, E. A. Paschos and G. Piranishvili, Phys. Rev. D **74**, 014009 (2006).
- [70] J. Liu, N. C. Mukhopadhyay and L. S. Zhang, Phys. Rev. C **52**, 1630 (1995).
- [71] T. R. Hemmert, B. R. Holstein and N. C. Mukhopadhyay, Phys. Rev. D **51**, 158 (1995).
- [72] S. L. Adler, Annals Phys. **50**, 189 (1968).
- [73] T. Kitagaki *et al.*, Phys. Rev. D **42**, 1331 (1990).
- [74] L. Tiator *et al.*, Eur. Phys. J. ST **198**, 141 (2011).
- [75] D. Drechsel, S. S. Kamalov and L. Tiator, Eur. Phys. J. A **34**, 69 (2007).
- [76] K. A. Olive *et al.* (Particle Data Group), Chin. Phys. C, **38**, 090001 (2014).
- [77] M. Pohl *et al.*, Phys. Lett. B **79**, 501 (1978).
- [78] C. E. Anderson [MiniBooNE Collaboration], AIP Conf. Proc. **1189**, 195 (2009).
- [79] S. Nakayama *et al.* [K2K Collaboration], Phys. Lett. B **619**, 255 (2005).
- [80] Y. Kurimoto *et al.* [SciBooNE Collaboration], Phys. Rev. D **81**, 033004 (2010).
- [81] E. Hernandez *et al.*, Phys. Rev. D **81**, 085046 (2010).
- [82] M. Lacombe *et al.*, Phys. Lett. B **101**, 139 (1981).